Internship report 2A ENSG

Documentation of a new vesuvianite deposit: gemological description of the material and its inclusions, origin of the color and variations observed, spectroscopic and chemical analyses.

Lola JOUGLA

Supervised by **Féodor BLUMENTRITT**

Academic supervisor**: Judith SAUSSE**

GGTL Laboratories Switzerland – HERESET SA

4Bis Route des Jeunes, CH-1227 Les Acacias, Geneva, Switzerland.

Analytical note

Title	Internship report 2A ENSG
Setting and nature of the work	Report of the study done during my 2A internship at GGTL Laboratories Switzerland in Geneva.
Dates of the beginning and the end	24/06/2024 – 30/08/2024
Autor	Lola JOUGLA
Date of the publication	September 2024
Supervisors	Féodor BLUMENTRITT and Judith SAUSSE
Summary	Documentation of a new vesuvianite deposit: gemological description of the material and its inclusions, origin of the color and variations observed, spectroscopic and chemical analyses.
Key words	Vesuvianite, gemology, spectroscopy, inclusions, colours, deposit, rodingites
Number of pages	41
Annexes	6

*I thank all the **GGTL team** for these 10 weeks, its kindly welcome and help during my researches. I thank especially my supervisor, **Féodor BLUMENTRITT** for his explanations and gaiety with me throughout these two months. Also, I want to thank **Franck NOTARI** for his help and his loan of vesuvianite samples, **Candice CAPLAN** for generously welcoming me in her company.*

*I thank **Judith SAUSSE**, my academic supervisor for her monitoring and her advices during my internship.*

Table of contents

Table of figures

Table of charts

Table of annexes

Introduction

The internship of my second year at the ENSG engineering school takes place at the GGTL Laboratories Switzerland – HERESET SA located at 4Bis Route des Jeunes, CH-1227 Les Acacias, Geneva, Switzerland. The company born in 2011 from the fusion between two laboratories: GemTechLab and Gemlab became today GGTL Laboratories Switzerland and Liechstenstein. The company is led by Candice CAPLAN and composed by 15 employees. This company includes a laboratory with various spectrometer (UV-Vis-NIR, FTIR, Raman, DFI) and X rays fluorescence spectrometer (EDXRF) and binocular loup are at disposition for observations. The team is divided into two groups, the diamond team and the coloured gems team whose I am. The first team, specialized in diamonds, has to identify natural diamonds from synthetic (Chemical Vapor Deposit CVD or High Pressure – High Temperature HPHT). This step is followed by a gradation to control the quality of the diamond, its purity, colours, fluorescence or symmetry to isolate diamonds which are different from customer demand. At the end, members of this team make a certification and resend the product. The other team, constitute especially of my supervisor Féodor BLUMENTRITT, does more chemical analyses to characterised the naturality or the origin of a coloured stone as emerald, sapphire or even pearl. They analyse if treatments have been done on the sample or not according to the demand of the customer. Finally, they also create a certificate which is resend to the customer. In parallel of these analyses, the gemmologists can also realise a research project on a precise subject, for instance about some rocks referenced in the Swiss Gems Data Foundation (SGDF) founded by the co-founder of GGTL, Franck NOTARI. This foundation was created six months ago and is mainly supplied by Mr. NOTARI but it will be supply by other donators in the future. This foundation, constituted by a lot of samples from the world, is reserved for gemological researches.

By the way, the company services concern the big institutions of horology and jewellery.

I - Context of the study

Within the scope of my internship, I have to study a new deposit of vesuvianite from Kunar Valley in Afghanistan and write an article about this subject. This one will be published in the *Journal of Gemmology* magazine which is an international British journal in the gemmological area. The aim of the study is to identify, characterize the material and its inclusions, the origin of the colours and make hypothesis about the geological context of the deposit. The particularity of gemmological area is that all of the methods use are non-destructive to keep customers' products intact. Besides, a large work of bibliographic researches was done to gather a maximum of information about the subject, to complete, confirm or contradict our results.

The name of the mineral, *vesuvianite* comes from Italy and more precisely Vesuvius mount. (Medenbach & Sussieck-Fornefeld 1982). According to Aksenov et al 2016, vesuvianite group consists in different element-rich species of vesuvianite as wiluite (Al/B-rich vesuvianite), fluorvesuvianite (F-rich vesuvianite), manganvesuvianite (Mn-rich vesuvianite), magnesievesuvianite (Mg-rich vesuvianite) and cyprine (Cu-rich vesuvianite). Vesuvianite minerals are complex tetragonal sorosilicates (www.mindat.org/min-4223.html) and the International Mineralogical Association (IMA) gives it the following chemical formula as an ideal formula: $Ca_{19}Fe^{3+}Al_4(Al_6Mg_2)(\square_4)\square[Si_2O_7]_4[(SiO_4)_{10}]O(OH)_9$.
Vesuvianite can also be seen under the name *Idocrase* but this name is not approved by the IMA unlike vesuvianite. This material is abundant in diverse regions of the world such as Italy (Abart 1995), India (Kobayashi & Kaneda 2010) or China (Patel 2007).

This study is interesting because few people have taken an interest in this mineral and even fewer with a gemological aspect. There are some gemological publications on this subject as the one of Renfro & Koivula 2017 where they have detailed a vesuvianite inclusion in ruby. Nevertheless, this lack of gemological interest is not completely justified because the suitable density, hardness and the various colours of vesuvianite (yellow, green, brown, violet) can make it a suitable material for jewellery.

The aim of this study is to analyse a vesuvianite set from Afghanistan. Note that this set was bought by Franck Notari, who is a customer of the mine dealer. Samples were sold as hydrogrossular but quickly reidentified as vesuvianite, grossular or combinations of both. This set belongs to the Swiss Gems Data

Foundation (SGDF). People can confuse hydrogrossular and vesuvianite because of their similarities on optical properties, structures and chemical compositions (Perraki et al 2010). Hydrogrossular and grossular in general are part of the garnet group. They are cubic nesosilicates and their chemical formula is simpler than vesuvianite: $Ca_3Al_2(SiO_4)$ (www.mindat.org/min-1755.html).

The set studied is from Kunar Valley new deposit more precisely from Afghanistan side (Figure 1). So, no study has been done on it. Kunar Valley is a large-scale valley which recovers a part of North-West-Afghanistan and North-East-Pakistan. This area is a suture zone between Eurasian and Indian plates at the origin of Himalaya chain. This event took place during the early Paleogene (Palaeocene) (Jalil et al 2023).

Figure 1: Kunar Valley localisation, origin of the vesuvianite (from Google Earth and modified by L. JOUGLA)

Firstly, some articles detailed vesuvianite chemical formula as the one of Groat et al 1992 or Smart et al 2023. In their publication, they define respectively vesuvianite formula as:

$$X_{19}Y_{13}Z_{18}T_{O\text{-}5}O_{68}W_{10}$$

Or simply: $X_{19}Y_{13}Z_{18}O_{68}W_{10}$

According to these articles, X sites are eight or nine coordinates ([8] or [9]), Y sites are five or six coordinates ([5] or [6]) and Z sites, four coordinates ([4]). W sites are anion sites, mono or di-anionic including, for instance, $O^{-}OH^{-}$ or F^{-}. Also, T sites detailed by Groat et al 1992 can include B which has a tetrahedral polyhedron that is to say a four coordinate. More precisely, X sites can be divided in four, X1, X2, X3, X4, Y and Z sites in three like Y1, Y2, Y3 and Z1, Z2, Z3. According to Groat et al 1992, many different elements can compose these sites. X sites include mostly Ca but it can be also Na, Ln, Pb, Sb, Bi or Ti. Note that X4 site is only occupied by the half (by Ca). Also, rare earth elements (REE) can occupy X sites because of substitutions with Ca. Y is composed mostly by Al in Y2 or Y3 sites but also Mg, Fe, Ti, Cr, Cu, Mn, Zn. Y1 sites include Fe, Cu, Zn, Mg an Y3 sites include Al, Mg, Fe, Ti. Then, Z sites are completely composed by Si. The same article defines various cationic even polyvalent substitutions including Y sites. For instance, we can have:

- $Mg^{2+} \leftrightarrow Fe^{2+}$
- $Fe^{3+} \leftrightarrow Al^{3+}$
- $Al^{3+} \leftrightarrow Ti^{4+}$
- $Mg^{2+} \leftrightarrow Al^{3+}$

At the end, we often have:

- $(Mg^{2+} + Fe^{2+} + Mn^{2+}) + Ti^{4+} \leftrightarrow 2(Al^{3+} + Fe^{3+})$

Generally, we can quote some major substitutions in vesuvianite:

- $Mg^{2+} + Ti^{4+} \leftrightarrow 2Al^{3+}$ (in Y3 sites)
- $Mg^{2+}(+Fe^{2+}) + OH^{-} \leftrightarrow Al^{3+}(+Fe^{3+}) + O^{2-}$

(in bore free − vesuvianite)

- $B^{3+} + Mg^{2+} \leftrightarrow 2H^{+} + Al^{3+}$ $(in\ X\ sites)$

Others minor substitutions are:

- $Na^{+} + Ti^{4+} \leftrightarrow Ca^{2+} + Al^{3+}$ (in X sites)
- $Ln^{3+} + Mg^{2+} \leftrightarrow Ca^{2+} + Al^{3+}$ $(in\ X\ sites)$
- $Na^{+} + Al^{3+} \leftrightarrow Ca^{2+} + Mg^{2+}$ $(in\ X\ sites)$

Furthermore, it is interesting to detail some correlations between elements. In fact, when B is incorporated in vesuvianite structure, it is linked with a loss of H. Then, OH is replaced by O. Also, it is interesting to quote the anticorrelation between Al and Mg, partly explained by their substitution reaction (see substitution reactions above).

Chemical analyses will highlight which elements compose our samples and which substitution reaction can take place.

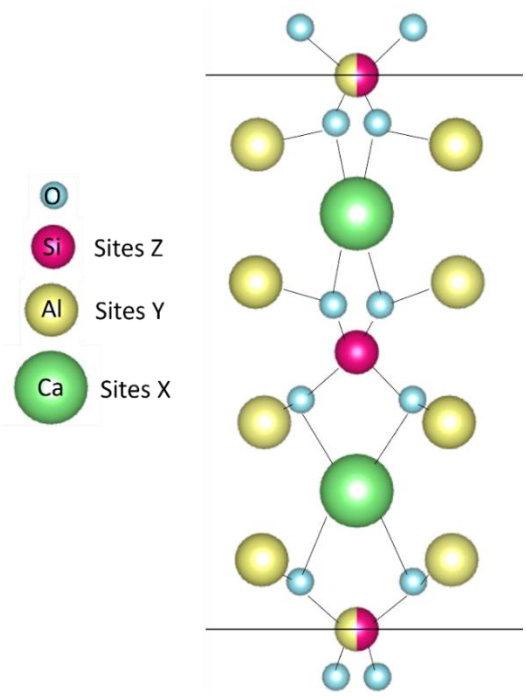

Figure 2: Crystalline structure of the site 1 of vesuvianite (from VESTA software and modified by L. JOUGLA)

The Figure 2 shows site 1 of the crystalline structure of vesuvianite (Fitzgerald et al 1986). This site is present two times in vesuvianite crystal and shows association between X, Y and Z sites in the structure.

Vesuvianite, with a tetragonal crystal system (www.mindat.org/min-4223.html), has a complex structure especially by its symmetry and space group. In fact, it can be various symmetries in different minerals as Smart et al 2023 explains. Vesuvianite can have P4/nnc space group but also P4/n or P4nc. Remember that P4 notation corresponds at a four axes symmetry. Additionally, these symmetries can be deducted by the setting up temperature of the mineral (Lu et al 2020 and Elmi et al 2011). In fact, some specific Raman peaks inform us about the crystallisation temperature of the mineral and consequently about the symmetry of the sample. This is the reason why Raman analyses can be very interesting. Note that a low temperature (~300°C-500°C) of crystallisation corresponds to a P4/n symmetry and a high temperature (>500°C) to a P4/nnc symmetry.

Besides, publications like Gaft et al 2015, Reisfeld et al 1996 and Czaja et al 2018 developpe the luminescence of vesuvianite for instance by iron, manganese or REE.

In this study, we characterise vesuvianite samples from Kunar Valley, spectroscopic and chemical analyses are done to identify the material, its inclusions and colour. Chemical formula but also its setting up and formation conditions will be detailed. This last part will deal with a geological aspect.

All of these researches aiming to understand vesuvianite structure and composition from this locality, two parameters that are commonly highly variable.

II - Materials and methods

A) Description of our samples

1) Gemological properties

27 samples from the set were chosen to do analyses series and have statistically reliable results. The aim being to have a number of various samples to analyse to see differences if there are. These samples, with mostly cabochon shape, were chosen macroscopically and under the binocular loupe regarding their colours, inclusions and fractures. This choice was done to have different colours, different inclusions, with fractures or not. Samples features are shown in Table 1.

Also, others samples SGDF-17910 and SGDF-17911 were **polished** (Figure 3) to have parallel faces thin enough (0.837mm and 0.658 mm) for IR absorbance and some Raman inclusions analyses.

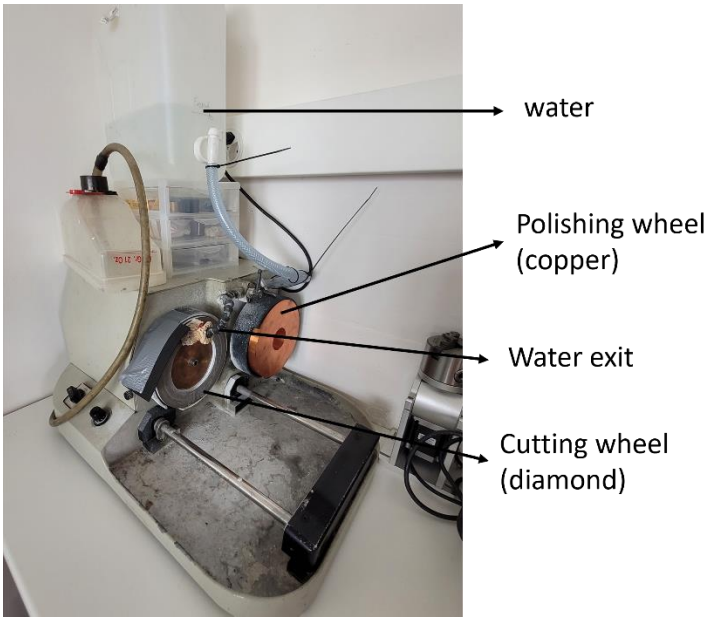

Figure 3: Polishing material (by L. Jougla)

References	Colours	Geographical origins	Shapes and cuttings	Masses (ct)	Sizes (Lenghts x Widths x thickness)(mm)
SGDF-16420	Brown-yellow	Pakistan	Oval cabochon	8,58	15,67 x 11,03 x 4,99
SGDF-16429	Pale green with dark green and white inclusions	Pakistan	Oval cabochon	19,82	20,05 x 14,84 x 7,07
SGDF-16255	Pale green with dark green and brown inclusions	Pakistan	Oval cut	4,91	14,55 x 10,92 x 3,93
SGDF-16430	Brown-green with dark green inclusions	Pakistan	Square cabochon	14,67	16,56 x 15,01 x 5,59
SGDF-16423	Half pale green, half green-turquoise	Pakistan	Oval cabochon	17,99	22,43 x 11,55 x 7,38
SGDF-16415	Half pale green, half brown	Pakistan	Oval cabochon	11,12	21,88 x 9,34 x 5,42
SGDF-16431	Pale green with dark green inclusions	Pakistan	Oval cabochon	17,86	21,38 x 14,66 x 6,59
SGDF-16433	Green-turquoise with dark green inclusions	Pakistan	Oval cabochon	14,56	19,2 x 11,43 x 6,59
SGDF-16428	Yellow-light brown	Pakistan	Circular cabochon	13,88	15,63 x 14,7 x 6,78
SGDF-16413	Green-white	Pakistan	Oval cabochon	9,78	19,93 x 8,85 x 6,22
SGDF-16424	Dark green with dark green and white inclusions	Pakistan	Oval cabochon	10,29	15,41 x 10,02 x 7,3
SGDF-16426	Green-light yellow	Pakistan	Circular cabochon	5,47	9,93 x 9,74 x 5,92
SGDF-16383	Brown-yellow	Pakistan	Oval cabochon	64,49	30,77 x 17,77 x 12,14
SGDF-16432	Brown-yellow with dark green inclusions	Pakistan	Oval cabochon	10,2	17,14 x 12,49 x 5,99
SGDF-16421	Apple green with dark green inclusions	Pakistan	Circular cabochon	19,5	18,82 x 16,7 x 7,19
SGDF-16302	Pale green with dark green and brown inclusions	Pakistan	Oval cut	9,18	14,73 x 12,06 x 7,48
SGDF-16414	Pale green with dark green inclusions	Pakistan	Oval cabochon	30,41	23,83 x 18,38 x 7,56
SGDF-16331	Brown	Pakistan	Barrel cut	8,37	14,85 x 8,77 x 6,99
SGDF-16419	Pale green with green-turquoise inclusions	Pakistan	Oval cabochon	12,78	17,05 x 12,48 x 7,13
SGDF-16422	Pale green with few black and brown inclusions	Pakistan	Oval cabochon	11,29	17,08 x 12,08 x 5,83
SGDF-16425	Pale green with dark green inclusions	Pakistan	Oval cabochon	4,4	13,15 x 8,7 x 4,45
SGDF-16417	Pale green with green-turquoise inclusions	Pakistan	Circular cabochon	8,87	12,85 x 12,81 x 6,14
SGDF-16418	Green-yellow with dark green inclusions	Pakistan	Drop cabochon	10,61	20,13 x 10,33 x 6,18
SGDF-16317	Pale green with many dark green inclusions	Pakistan	Oval cabochon	16,11	25,8 x 11,83 x 5,74
SGDF-16427	Green-ligth yellow	Pakistan	Pear cabochon	8,71	14,55 x 10,81 x 6,22
SGDF-16272	Brown-yellow	Pakistan	Oval cut	4,22	10,85 x 10,2 x 4,48
SGDF-16416	Pale apple green	Pakistan	Oval cabochon	16,73	21,44 x 12,33 x 7,36
INDE 6721	Apple green	India	Trillion cut	3,03	9,72 x 9,72 x 5,2
INDE 6722	Apple green	India	Oval cut	2,83	10,01 x 8,18 x 4,94
INDE 15039	Apple green	India	Oval cabochon	6,77	13,75 x 9,91 x 5,25
INDE 6708 -Petite-	Apple green	India	Oval cabochon	6,8	8,87 x 7,23 x 4,12
RUSSIE 4746	Green-white	Russia	Drop cabochon	1,52	9,08 x 6,51 x 3,5

Table 1 : Features and photographies of our samples (by L. JOUGLA)

In order to describe the gemological properties of the samples, **refraction and birefringence index** are measured with a Gem-A instrument refractometer with high refractive index liquid (Figure 4). Note that birefringence cannot be measured in polycrystalline and/or cryptocrystalline sample since orientations of crystallites are random.

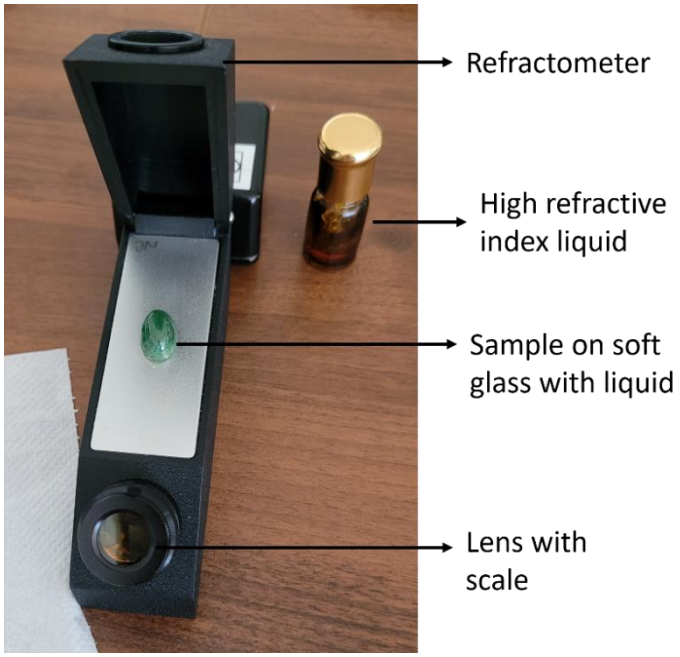

Figure 4: Refractometer (by L. Jougla)

Also, the **hydrostatic weighing** gives us a specific mass for our 27 samples with one weighing in the air (ma) and one weighing in the water (mw). The following calculate is used to have the specific masses:

$$Specific\ mass = \frac{ma}{ma - mw}$$

2) Gemological descriptions

Microscopic examination and micrographs collected in white light were performed using a Leica M165 C binocular microscope with integrated analyser, equipped with a DMC 5400 camera, in z-stack mode with parallax error compensation. The illuminators used (darkfield and brightfield) are GGTL Laboratories Switzerland models on a modified Schott base, with MC1500 dual controller (Figure 5).

Scale of micrographs are calculated taking into account the magnification and optics of the microscope. Values and constants are given by Leica user manual corresponding to the M165C model.

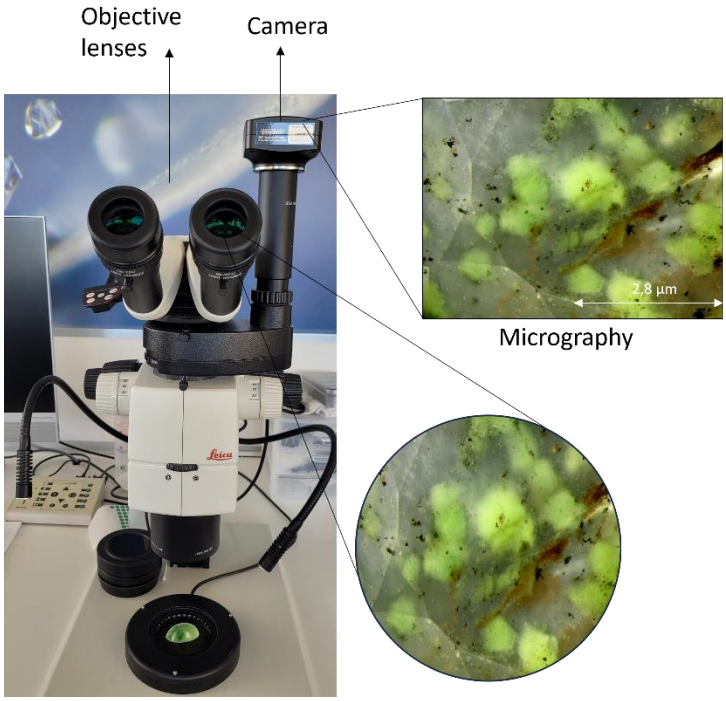

Figure 5: Principle of microcraphy on a binocular loup (by L. Jougla)

A gemological description of the colours is done by **gradation**. To do that, we use two colour references books, the *World of Color* and *Color Codex (*Figure 6*).*

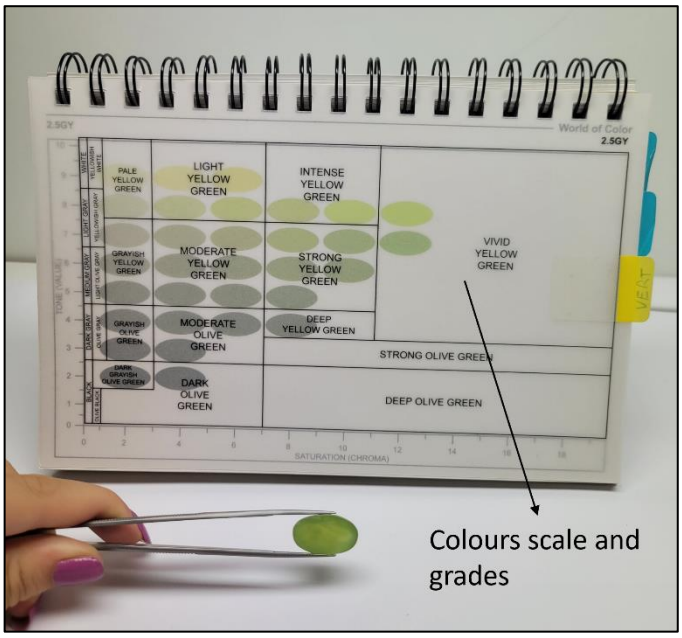

Figure 6: Colour gradation of the samples using Worl of Color reference booklet (by L. Jougla)

B) Samples identifications

From this part, methods are used to characterize and identify the material and not to describe the sample as previously.

Fourier transform infrared spectrometry was performed using a Thermo Scientific iS50 spectrometer equipped with a tungsten-halogen source, a La-DTGS-KBr detector (12500-350 cm-1), an XT-KBr separator and a rotating ZnSe polariser. The accessory used was a Spectratech Collector II for diffuse reflectance, modified for transmittance. The spectra were collected with 300 scans, and after a background of 20 scans, the FWHMs were calculated (Figure 7).

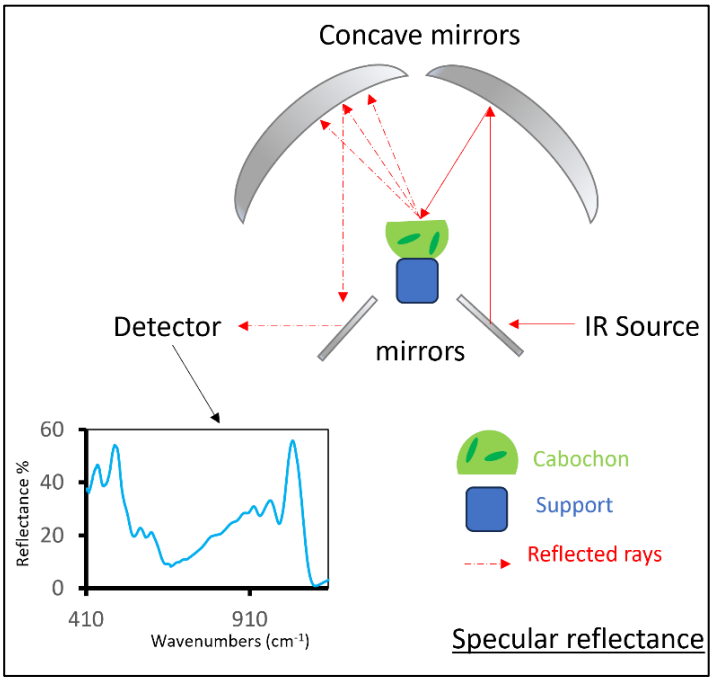

Figure 7 : Principle diagram of Specular Reflectance (by L. Jougla)

Raman spectra were acquired on a Thermo Scientific DXR3 Raman Microscope equipped with a 532 nm laser (max. power 10 mW). Several objective lenses are used either to analyse the surface of the sample for identification of the sample (x10 objective) or for identification of some inclusions (x10 or x20 objective). Depending of the intensity of the signal spectra are a minimum mean of 100 scans of 1s each but some spectra on inclusions are the accumulation of up to 4000 scans. Two different grating allow the acquisition on a usual range (100-3600 cm^{-1}) or extended range (100-6400 cm^{-1}).

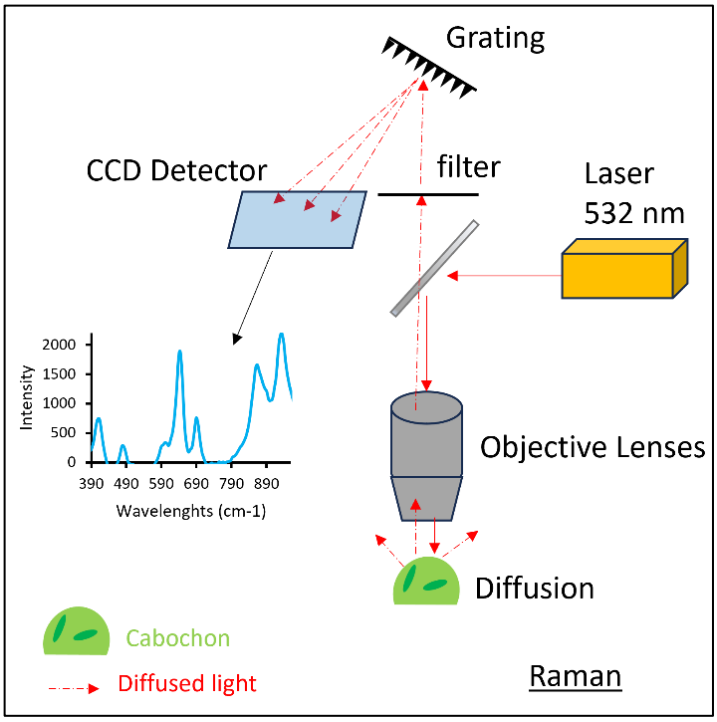

Figure 8: Principle diagram of Raman (by L. Jougla)

C) Composition analyses

EDXRF chemical analyses were performed on a ThermoFisher Scientific ARL Quant'X system, equipped with a Rh X-ray photon tube for excitation and a 1000 µm thick silicon drift detector electrically cooled by Peltier effect (three-stage module generating a λ of ≈ 120 °C), in normalized all-element analysis (Na → U), with 300 seconds of real acquisition time per condition (9 filters), in vacuum for light elements. Measurements were carried out on the stone table, with optimal geometry (± ≈ 1°) in relation to the angle of incidence of the excitation beam with the table (Θ = 45°), as well as with the detector (same Θ), samples on Prolene® film 4µm, analysed in rotation to reduce diffraction artefacts and analyse a defined round area of 7mm (Figure 9).

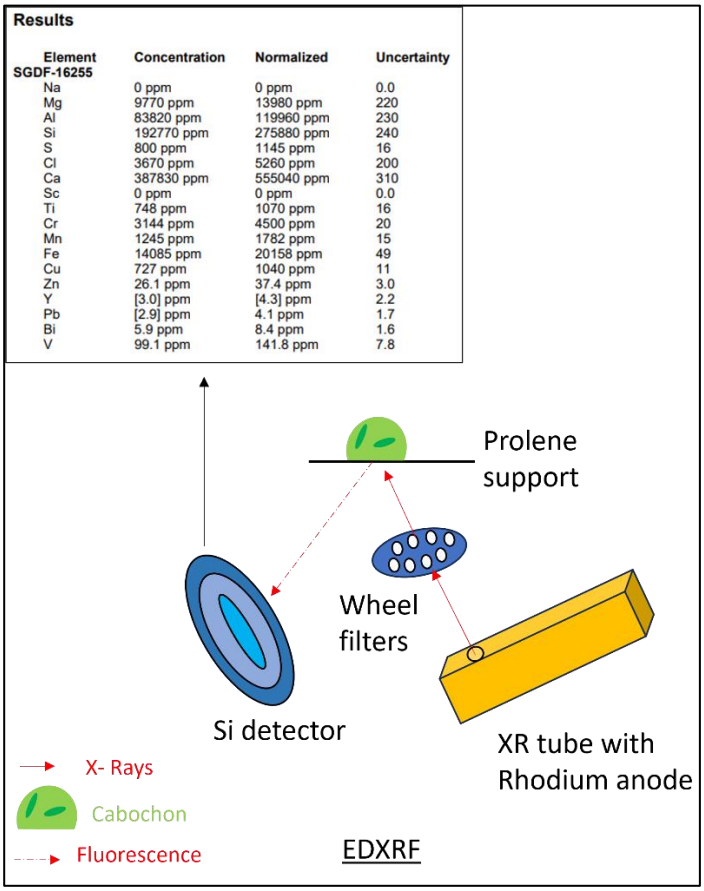

Figure 9: Principle diagramm of EDXRF (by L. Jougla)

D) Colour analyses

Ultraviolet-visible-near infrared (UV-Vis-NIR) transmission spectra were acquired on all the selected samples in the 300–1050 nm range using a custom-made four-channel spectrometer equipped with three Peltier-cooled CCD detectors.

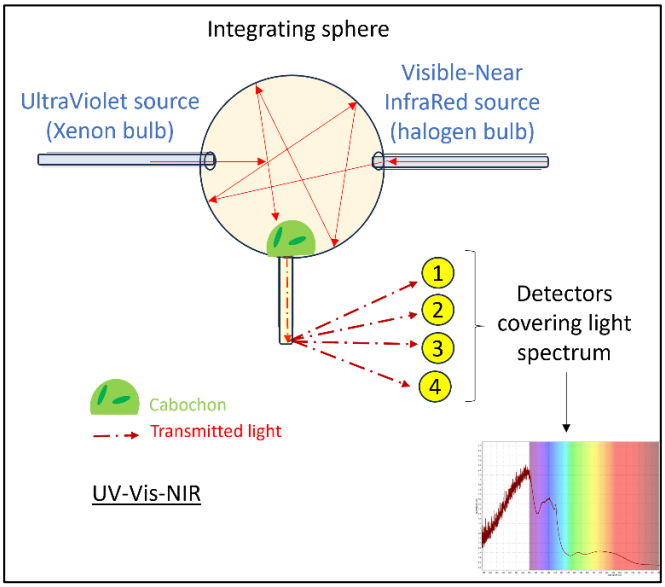

Figure 10: Principle diagram of UV-Vis-NIR (by L. Jougla)

E) Luminescence

Luminescence analyses (spectra and imaging) of these vesuvianites were carried out using two GGTL Laboratories DFI systems, model V2 and V3R, equipped with a 300W xenon source, filtered (6 filters from 200 to 400 nm) and focused, a single-channel spectrometer (resolution ≈- 1. 3 nm) for the V2R and two servo spectrometers with a resolution of ≈ 0.35 nm in the 350-850 nm spectral range and ≈ 0.7 nm in the 595-1190 nm spectral range, all cooled by Peltier effect (5°C), a 300 mW 405 nm laser source, filtered and focused. Imaging was carried out using a Leica DMC 4500 camera for V2 and a Sony IMX183/20GB for V3R, with a primary 100/50/100% observer/camera and secondary 100/100% camera/fibre spectrometer splitter. A GGTL Laboratories low-temperature accessory enables spectra to be collected at 77K (sample in contact with liquid N2 at -196°C) (Figure 11 and Figure 12).

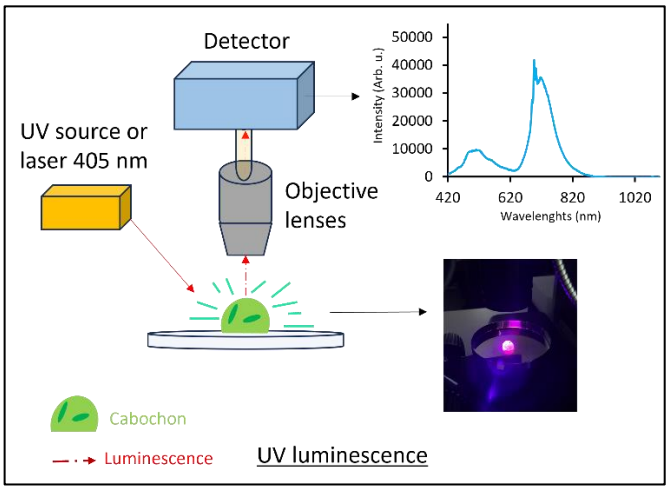

Figure 11: Principle diagram of UV-luminescence (by L. Jougla)

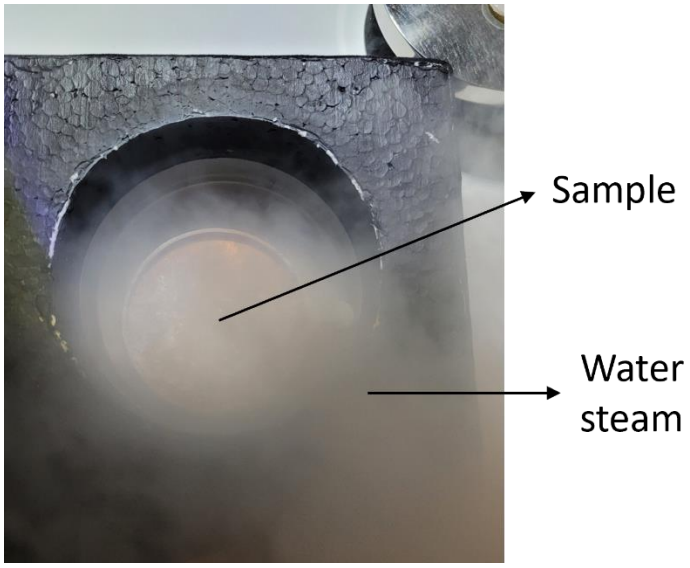

Figure 12: Luminescence analyses at low-temperature with liquid nitrogen (by L. Jougla)

III - Results and interpretations

A) Gemological properties

It was difficult to measure a **refraction** index on our cabochons, in fact, no line appeared on the refractometer scale because of the shape. There is only the index line of the liquid (~1.785). We can see this difficulty on the Figure 13. Nevertheless, it is possible to have an index when the measure is done on cut samples with facets thank to the flat part. On the four samples with facets, four measures are realised for each sample. There are SGDF-16255, SGDF-16302, SGDF-16272 and SGDF-16331 samples. In this way, the average value of 16 measures is 1.708 [1.705 – 1.713].

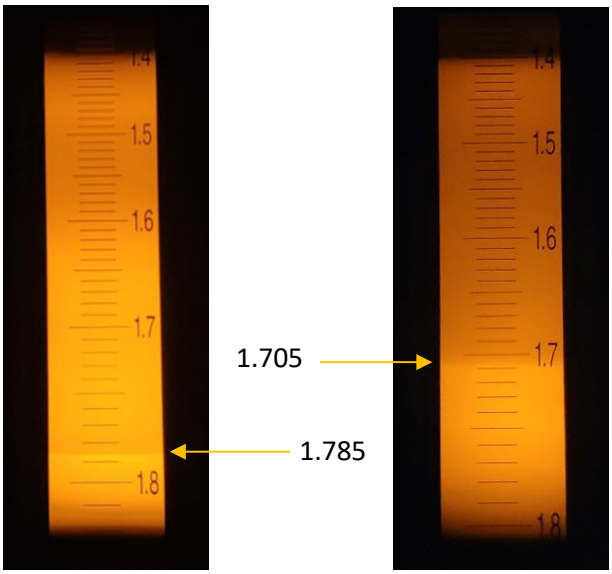

Figure 13: Refractometer values (by L. JOUGLA)

Besides, **gradation of colours** was done with the *World of Color* and the *Color Codex* reference books. Color Codex is better adapted to cut stone than cabochons since it reproduces aspects of reflections on facets. Six samples, with different colours are characterized, they are the same which will be developed later, in the 1) UV-Vis-NIR spectroscopy part. Firstly, and according to the World of Color and our observations, SGDF-16429 has a greenish white colour on one side and a light yellowish on another. SGDF-16331 (facetted) is light greenish yellow and its reference by the Color Codex is 50-03. Also, SGDF-16383 is characterized as vivid greenish yellow while SGDF-16427 is pale yellow green. Furthermore, we can qualify SGDF-16416 as light-yellow green and SGDF-16433 as light

yellowish green. The comparisons between sample and colours grades are shown in Annexe 1.

Macroscopically, these results allow us to say that our 27 samples cover a large scale of colours. Property which interests a lot the gemologists concerning jewellery creation.

Furthermore, **specific masses** of samples have been measured. Results are shown in the Annexe 2. The average value of the 27 measures is 3.374 ct [3.306 – 3.563]. This property confirms the identity of vesuvianite comparing with bibliography values. In fact, our value coincides which the scale given by M. Manutchehr-Danai 2005, namely between 3.33 and 3.45.

Also, **lustre** of the samples is characterized. Choices of this property is done by comparison with others materials knowing their lustres. The Annexe 2 highlights this scale of lustres. Our samples are represented by SGDF-16419 which is a representative cabochon of the bundle. In conclusion, our samples have a bright vitreous lustre as almandine pyrope or good grade polished chalcedony.

B) Gemological descriptions, inclusions

The session of micrographies conducted with a binocular loupe allowed us to identify various characteristics of our samples. The matrix exhibits a colour ranging from yellowish to green to more or less intense brown. Different inclusions are visible:

- **Green inclusions**, mostly automorphic (in about 80% of our samples), with a cloudy aspect but visibly prismatic, pentagonal, or even hexagonal in some (SGDF-16424). However, in a few samples, these green inclusions can appear more circular or rounded (SGDF-16317) (Figure 14).

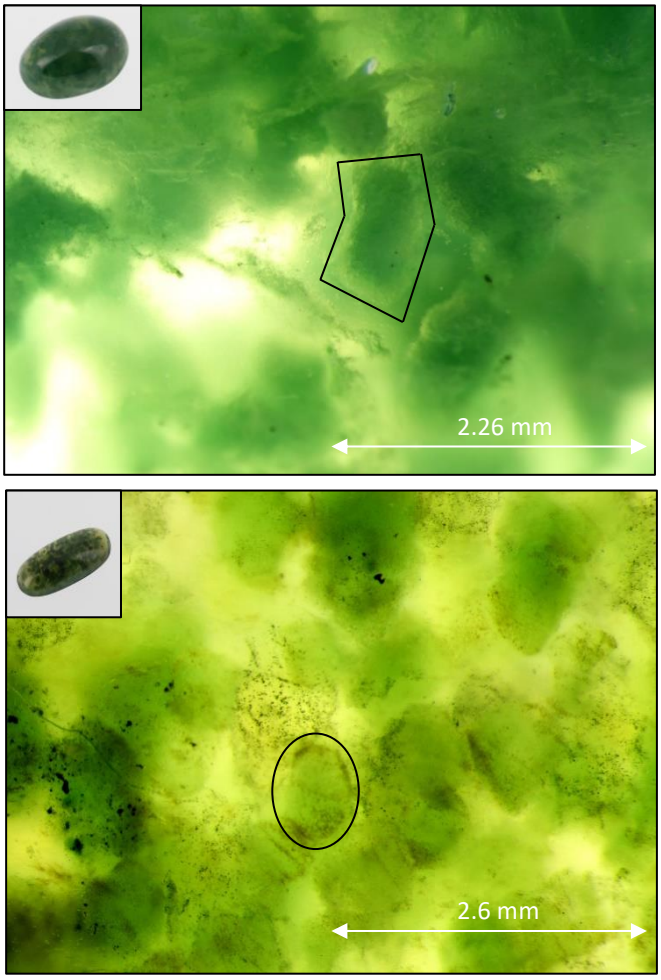

Figure 14: Examples of green inclusions in SGDF-16424 and SGDF-16317 (photographies by L. JOUGLA)

- **Black inclusions** in the form of more or less large clusters, more or less numerous, xenomorphic and sometimes automorphic. Present in the majority of samples: 22/27, or 81% of our batch. These black clusters are associated with the green inclusions/crystals mentioned earlier, most often located on the periphery of this latter and sometimes covering the same area (SGDF-16302). These black inclusions can also form a veil-like appearance on the structure (SGDF-16425 and SGDF-16317). Note that the coarsest clusters can be observed macroscopically (Figure 15).

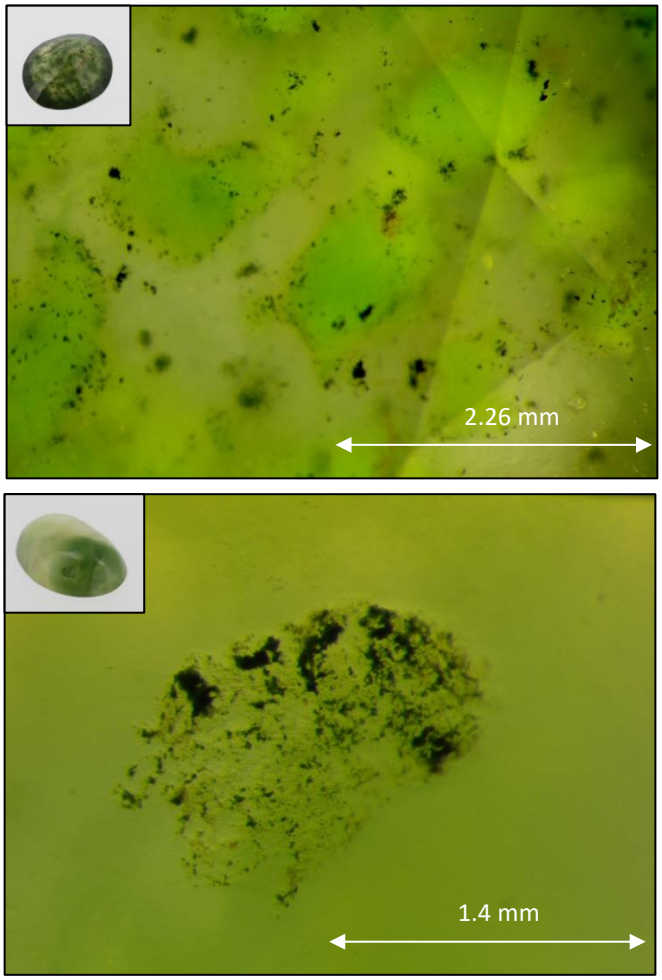

Figure 15: Examples of black xenomorphic inclusions in SGDF-16302 and SGDF-16425 (photographies by L. JOUGLA)

- **Brown inclusions**, can be light (SGDF-16302) to intense (SGDF-16415) when in clusters. These have a fairly dendritic shape (SGDF-16432) and are present in 67% of our samples. This shape indicates a rapid growth of the inclusion where it did not have time to crystallize automorphically (Sunagawa 2005). This may indicate a sudden change in conditions in the environment, whether physical (pressure, temperature) or chemical (Redox, acid-base). It is also possible that the fluid carrying the components of these inclusions infiltrated through zones of weakness, causing this specific shape (Figure 16).

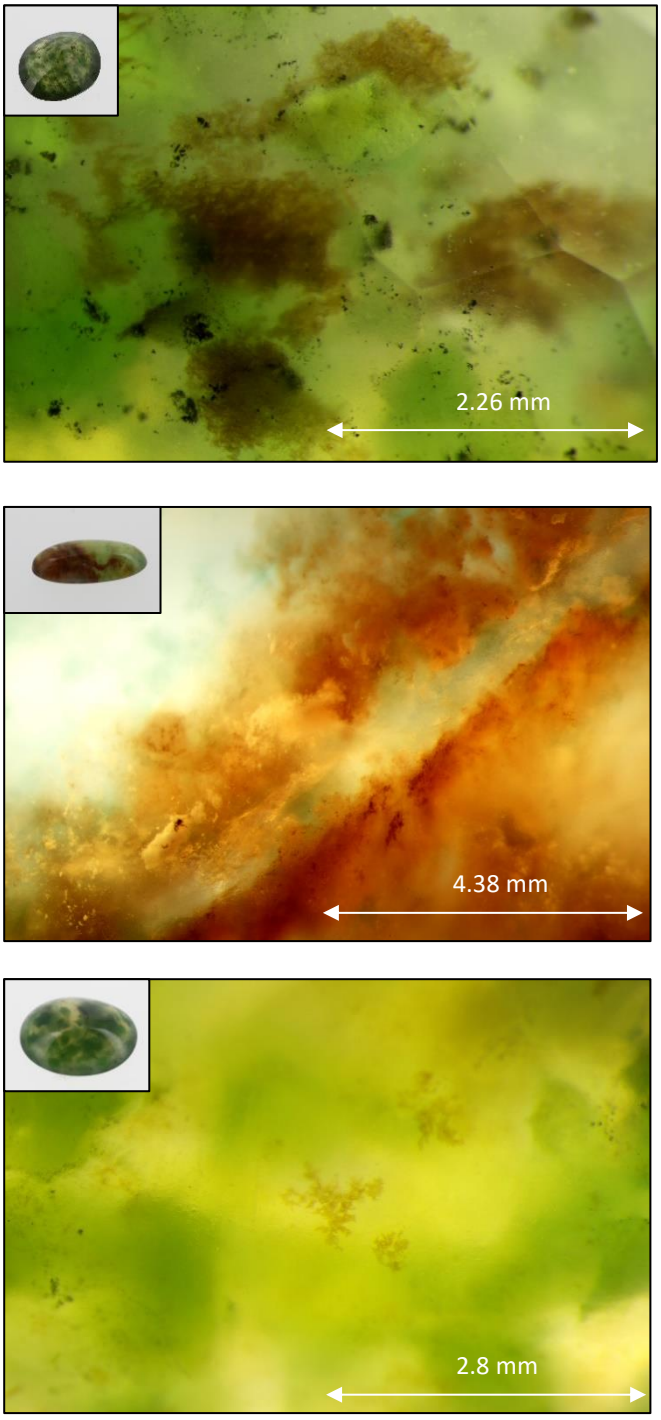

Figure 16 : Brownish inclusions in SGDF-16302, SGDF-16415 and SGDF-16433 (photographies by L. Jougla)

- **White inclusions**, very small in size, scattered (resembling dots) or in clusters and subautomorphic (SGDF-16255 and SGDF-16420), present in almost all our samples (21/27 or 78%). Note that these inclusions are the only ones present in our samples with a translucent appearance and no observable macroscopic inclusions (Figure 17).

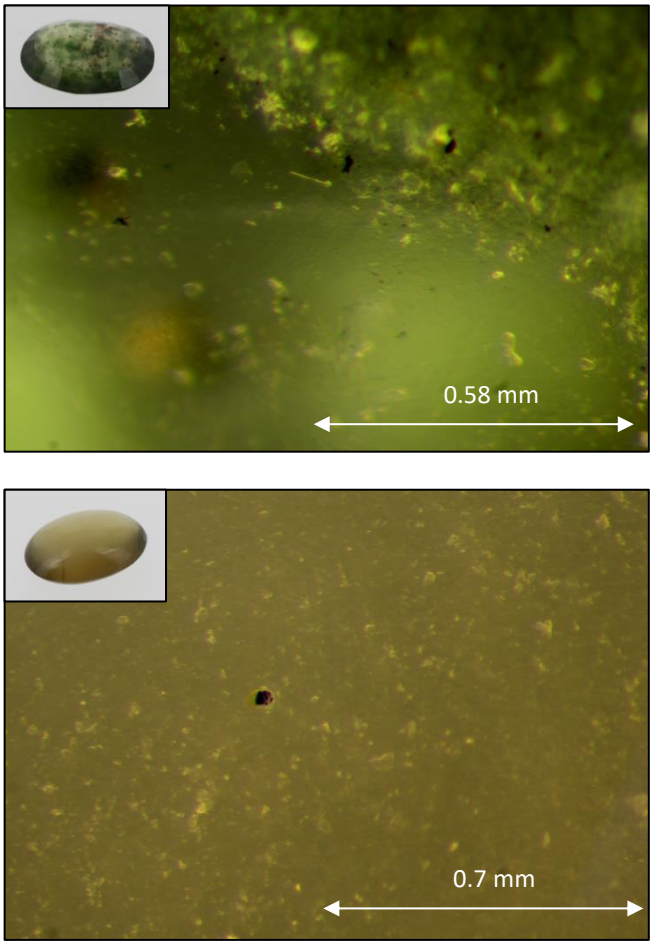

Figure 17: Dotted inclusions in SGDF-16255 and SGDF-16420 (photographies by L. Jougla)

- Variable-colored inclusions (whitish to green), **filamentous** like veils or ghosts, difficult to quantify. These are often oriented in the same direction. This oriented growth indicates pressure conditions favorable to the establishment of stresses. Note that some of these clear inclusions are oriented parallel to fractures, as illustrated by sample SGDF-16417 (Figure 18).

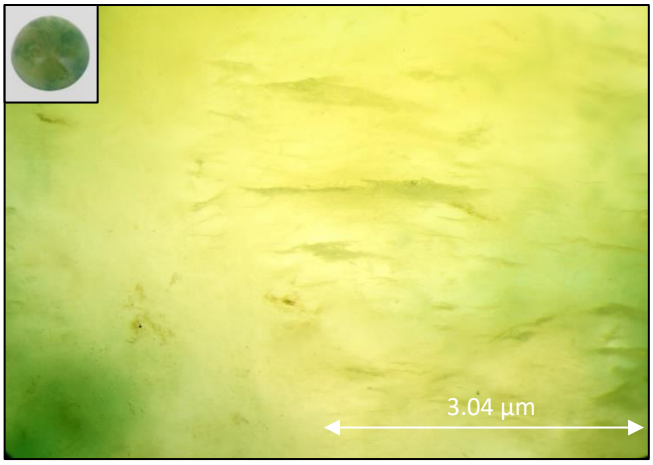

Figure 18: Filamentous inclusions in SGDF-16417 (photography by L. JOUGLA)

- **Golden inclusions**, are observed quite clearly in some samples as SGDF-16302. It is xenomorphic, resembling a cluster, and sometimes it is seen in association with the black inclusions described earlier. The latter are found within our golden inclusions. This, by the principle of inclusion, means that these black structures are older than the golden structures that grew around them (Figure 19).

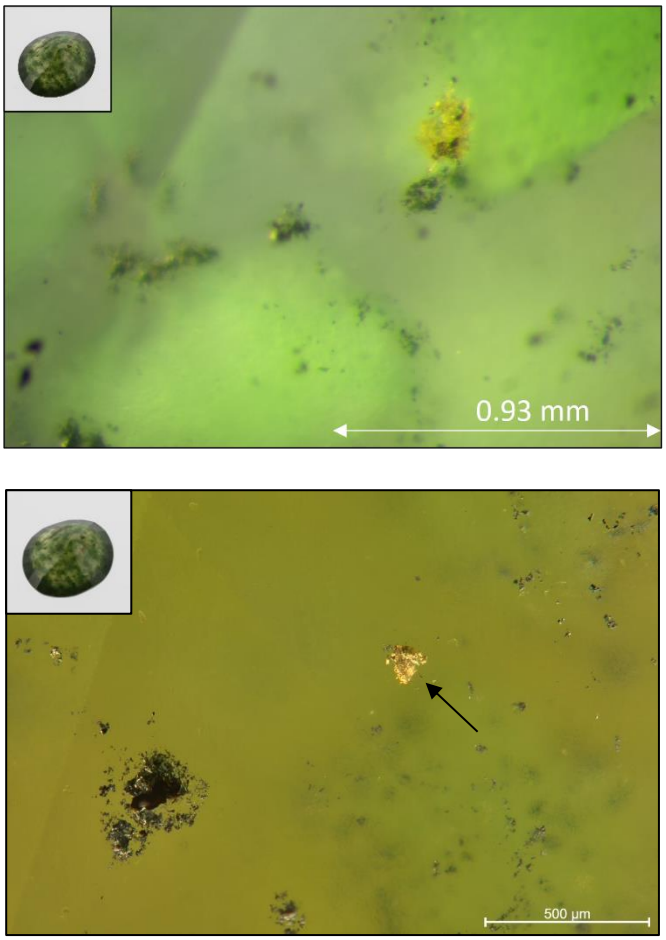

Figure 19 : Golden inclusion in a black inclusion in SGDF-16302 (photography by L. Jougla) and Golden inclusion and black automorphic inclusion in SGDF-16302 (photography by F. BLUMENTRITT)

Moreover, we can note that a number of our samples are fractured. Some of these fractures can be seen macroscopically (SGDF-16417) while others are visible under the binocular loupe (SGDF-16431) (Figure 20 and Figure 21).

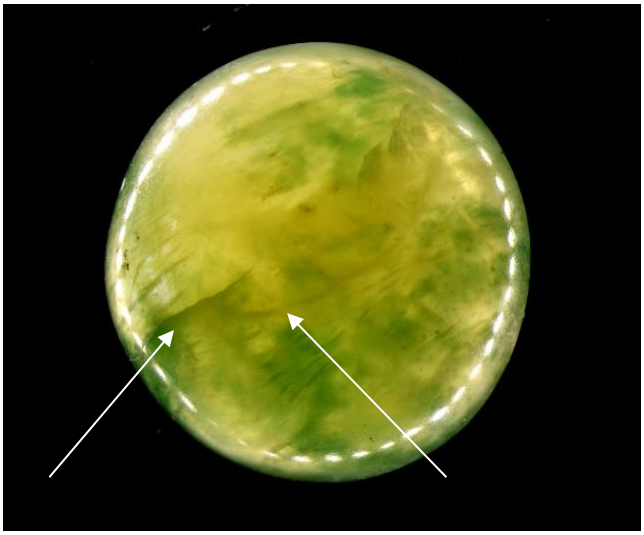

Figure 20: Fractures seen in SGDF-16417 under binocular loup (photography by L. JOUGLA)

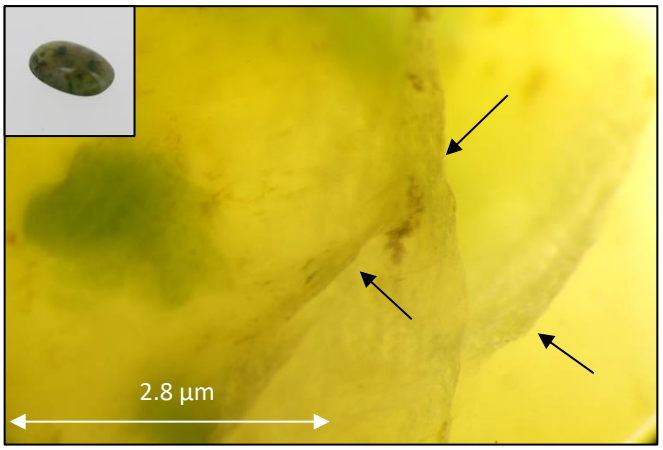

Figure 21: Fractures of SGDF-16431 (photography by L. JOUGLA)

The crossed polariser allows us to see irisations in the structure. These ones highlight potential deviations of the light rays showing irregularities in the crystallin structure. On the Figure 22 it is possible to see irisation differences between crossed or parallel polarisers. These irisations could correspond to structural tensions or fluid inclusions pointing out anomalies in the mineral structure.

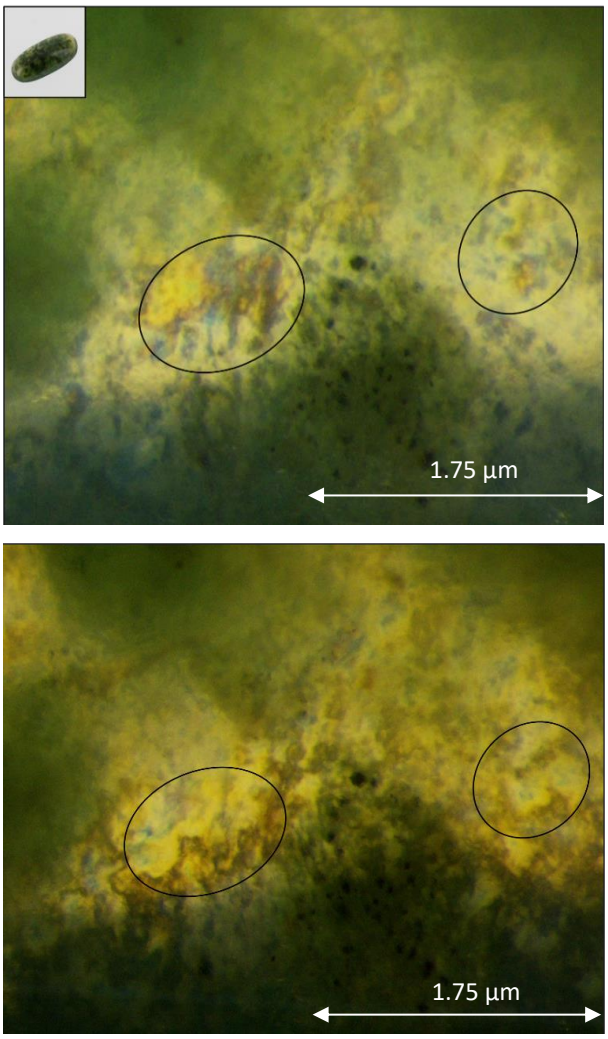

Figure 22 : Fluid inclusions in SGDF-16317, differences seen under cross polarizers (photography by L. JOUGLA)

C) Inclusions identifications with Raman spectrometer

The Raman spectrometer is used to identify the materials and especially inclusions in our vesuvianites. Using a laser, inclusions can be aimed for analyses. Six various inclusions have been identified whose five are mineral materials.

-Firstly, **grossular** was noticed by analyses. In fact, SGDF-16302's inclusion is automorphous and with a green colour. Raman identified it as grossular, that is to say as material with calcium, aluminium and silicium (www.mindat.org/min-1755.html). It is consistent because SGDF-16302 sample has the maximum quantification of calcium among all our vesuvianite samples. Aluminium and silicium are also on sufficient quantities in this sample. It is not surprising to see

grossular as inclusions in vesuvianite as the view of their similarities.

-Then, **clinochlore** was also remarked by the Raman. Its chemical formula is $Mg_5Al(AlSi_3O_{10})(OH)_8$ (www.mindat.org/min-1070.html). By the way, it is very rich in magnesium. This element is in notable quantities in samples where clinochlore was found namely SGDF-16424 and SGDF-16432 (see chemical analyses below). These inclusions are either automorphous with a trapezoid shape and colourful or automorphous black inclusions. On Raman clinochlore spectrum, one peak is remarkable at ~679 cm^{-1} which can be associate at a Si-O-Si liaisons in clinochlore (Lu et al 2020). Furthermore, according to Lu et al 2020, iron and chromium substitutions in octahedrally coordination of clinochlore, decrease the transparency of the sample.

- Furthermore, **covellite** was found as inclusion in vesuvianite. This copper sulphur (www.mindat.org/min-1144.html), CuS, was found in SGDF-16302 sample for two times. At each time, the inclusion appears cubic and metallic with blue aspect. The spectrum is clear and the identification reliable. As covellite reference spectrum we have the major peak at ~470 cm^{-1}. The chemical quantification confirms the presence of copper in this sample. In fact, according to our chemical results, SGDF-16302 sample is one of the two samples with copper

- **Magnesiochromite** was also identified by Raman. Its chemical formula is $MgCr_2O_4$ (www.mindat.org/min-2493.html). The inclusion has a prismatic shape and a black colour. Magnesiochromite was found in SGDF-16432 vesuvianite sample. This one has high quantification of magnesium and chromium (made by chemical analyses developed below) compared to others, which confirm this possible identification.

- Moreover, **Amesite** is present as inclusion in SGDF-17910 sample. The chemical formula of this mineral is $Mg_2Al(AlSiO_5)(OH)_4$ (www.mindat.org/min-197.html). With the same composition than clinochlore, amesite is often founded in association with this mineral. By the way, it is not surprising to found this silicate in some samples. This inclusion is brownish with a dendritic shape. This type of inclusion was only identified in this sample, certainly because of its weak thickness. In fact, we have polished the sample SGDF-17910 to have less deepness to better see the inclusions.

-Finally, **amorphous carbon** has been in this same sample. In fact, black inclusions like stains were noticed has amorphous carbon because spectra show two large band at ~1350 cm^{-1} and ~1600 cm^{-1}. We can see these bands on Figure 23. By definition, this carbon is not well crystallized and is characterized by these two bands (Ferrari & Robertson 2000). This inclusion may be amorphous graphite carbon (sometimes mentioned as disordered graphite in the literature).

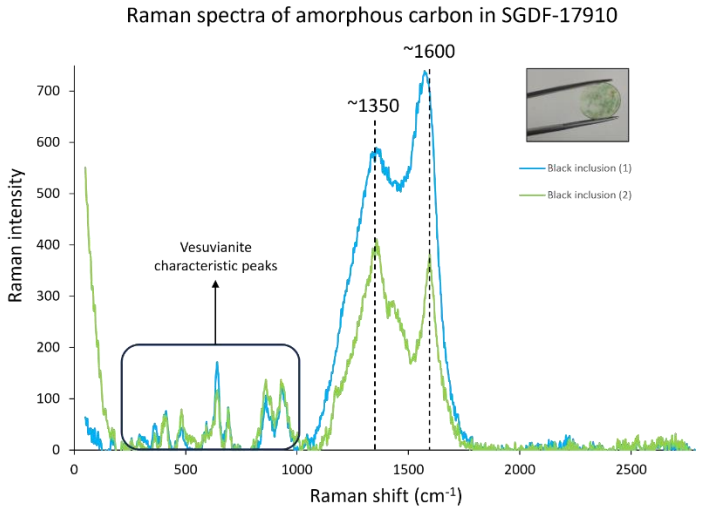

Figure 23 : Raman spectra of two inclusions of amorphous carbon in SGDF-17910

Nevertheless, some inclusions described in the precedent part could not be identified. In fact, white inclusions as dots or filaments and the gold inclusions have been identified as vesuvianite. Some of them, being certainly not vesuvianite as the simple view of the colour (gold) could have been characterized as it because of the large thickness of samples composed of them. Raman laser has not reached precisely the inclusion, and, by the way, analysed the vesuvianite matrix crystals.

D) Materials identifications

1) Identification of our samples

One of the first analyses we have to do is to verify the identification of our 27 samples. To do so, we used infrared and Raman spectroscopy which characterize the material through their atomic vibration modes. Note that we use some vesuvianite samples as references for IR spectroscopy analyses to strengthen the reliability of the results. These last originate from India or Russia.

a) IR spectroscopy

- Reflectance measures

Analyses of our 27 samples were realised and the results are as follows. Firstly, we interested us at 23 IR-spectra, then, spectra of SGDF-16426, SGDF-16427, SGDF-16428 and SGDF-16429 will be detailed. Spectra of the 23 samples are very similar so, the following illustration (Figure 24) gives three representative spectra examples of these 23, compared with our vesuvianite reference INDE 6722. It is possible to note three absorption band that are shared by our samples and the reference. A small band is measured at ~460 cm^{-1} followed by two others, one smaller and one approximately with the same reflectance value. These ones occur at ~940 and ~1000 cm^{-1} and are present on the four spectra. Another small variation, but noticeable in every spectrum of the illustration, is present at ~1260cm^{-1}. All of these common characteristics make, by comparation with INDE 6722 and by the data base, our 23 samples as vesuvianite.

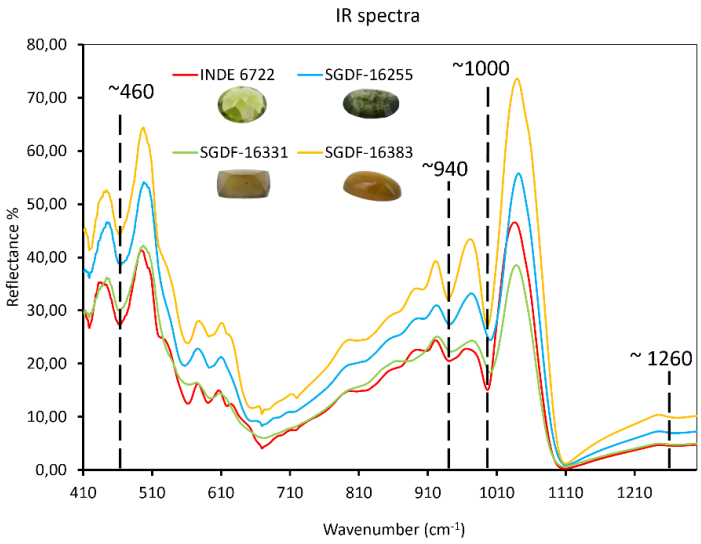

Figure 24: IR spectra of some vesuvianite samples

It is also interesting to say that spectra show characteristic peaks of water, sebum and carbon dioxide due to our manipulations and the environment (Annexe 4).

Nevertheless, as we said previously, four samples' spectra show differences with the vesuvianite reference. These results are shown in the Figure 25. Even if some bands are shared by all the five samples as the one at ~490cm^{-1}, SGDF-16426, SGDF-16427, SGDF-16428 and SGDF-16429 have two more bands at ~530 cm^{-1} and ~890cm^{-1}. We can precise that the last one is an absorption band. Furthermore, another band is a little specific because it is present in the spectra of SGDF-16426, SGDF-16427, SGDF-16428 and INDE 6722. In fact, the significant peak at ~1030cm^{-1} is not visible in SGDF-16429 spectrum (in pink). By comparison with precedent references registered, the data base of GGTL Laboratories characterizes this sample as grossular. At the contrary, SGDF-16426, SGDF-16427 and SGDF-16428 are identified as vesuvianite.

Hence, it is possible to say that these last three may be transitional samples with intergrown vesuvianite and grossular crystals. It would be the reason why their spectra have two peaks shared with vesuvianite and two peaks shared with grossular.

Thus, grossular can be differentiate from vesuvianite by the presence of small absorption bands at ~530 cm^{-1} and ~890 cm^{-1}, and the lack of the high band at ~1030 cm^{-1}.

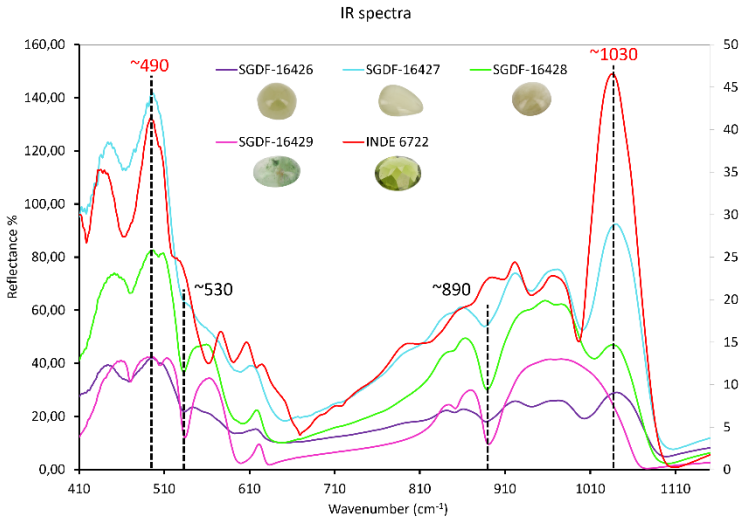

Figure 25: IR spectra of grossular and transitional samples from our bundle

- Absorbance measures

After the polishing of the sample SGDF-17911 to have two parallel faces with a thickness of 0.658 mm, IR absorbance can be done. Others samples are too thick and their spectra is mainly recorded with total absorption.

The article written by Paluszkiewicz & Zabinski 2004 details vesuvianite IR absorbance spectra. They said some absorption bands are characteristic to low or high temperature vesuvianite.

It is necessary to precise that vesuvianite which crystalized at a temperature <500°C (~300°C-500°C) are considered as low temperature vesuvianite and these which crystalized at a temperature >500°C as high temperature vesuvianite (Kobayashi & Kaneda 2010). Another source, Elmi et al 2011, associates low vesuvianite at a crystallization temperature <300°C.

According to Paluszkiewicz & Zabinski 2004, the presence of 7096 cm^{-1} and 7170 cm^{-1} bands on the spectrum corresponds to low-temperature vesuvianite. These absorption peaks can be seen in our sample as the Figure 26 shown. More precisely, our peaks are at ~7108 cm^{-1} and ~7170cm^{-1}.

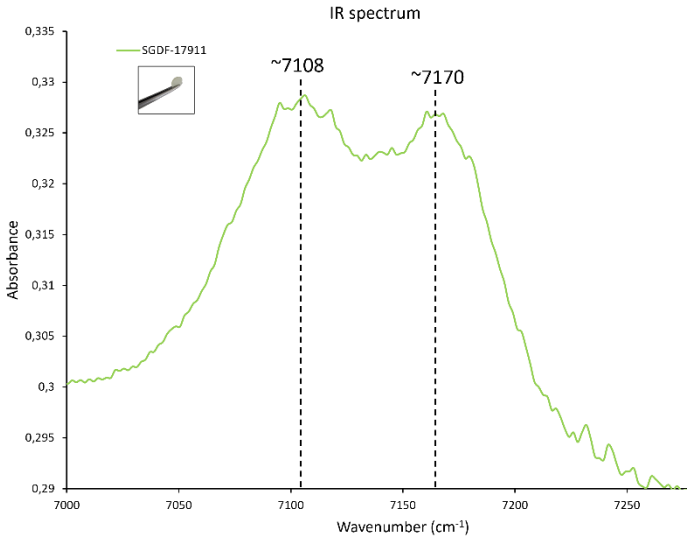

Figure 26: SGDF-17911 IR spectrum, two characteristic peaks

Therefore, these two peaks inform us that SGDF-17911 which is representative of our vesuvianite, was setting up at low-temperature especially as high temperature bands quoted by the article are no present in our spectrum.

Moreover, it is interesting to remarks two others absorption bands in SGDF-17911 spectrum. In fact, we can see two peaks at ~5006 cm^{-1} and ~5095 cm^{-1}. These absorption bands are not interpreted in the article but we can make the hypothesis they are characteristic of low-temperature vesuvianite (Figure 27).

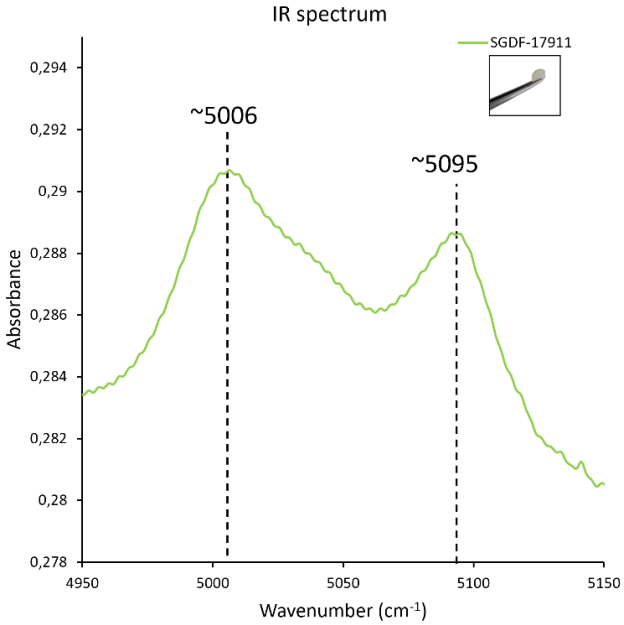

Figure 27: SGDF-17911 spectrum, others remarkable peaks

b) *Raman spectroscopy*

- Mineral identifications

Our 27 samples were put in the Raman spectrometer in order to confirm or deny IR results about our samples identity.

23 of the samples have a similar Raman spectrum. In fact, there is a small and large band at ~410 cm^{-1} and two consecutive peaks at ~640 cm^{-1} and ~690 cm^{-1}. The ~640 is higher and finer than the ~690 which is similar to the ~410. There is also another wider and more intense band than ~410 cm^{-1} and ~690 cm^{-1}, at ~860 cm^{-1}. A last recognizable peak, more intense and wider than ~640 cm^{-1} is present at ~935 cm^{-1} (Figure 28).

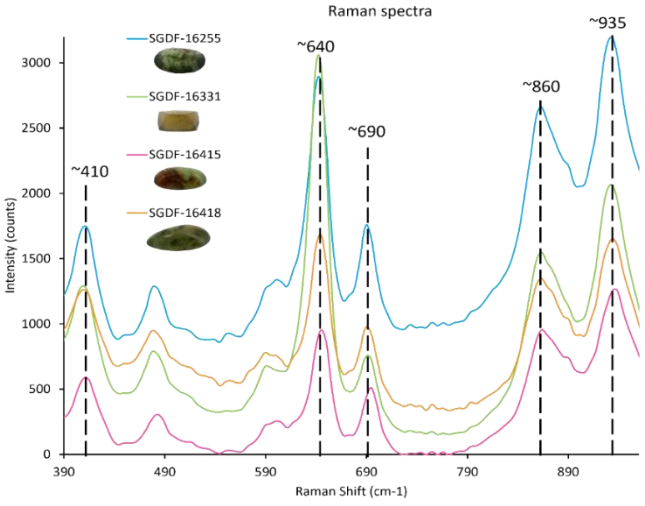

Figure 28: Vesuvianite Raman spectra

Furthermore, a large doublet is visible at ~3639 cm^{-1} and ~3675 cm^{-1} on every spectrum, with various shapes and intensities as we can see in the Figure 29.

For these 23 samples, the data base of the Raman spectrometer (RRUFF) analyses them as vesuvianite which confirms the IR results.

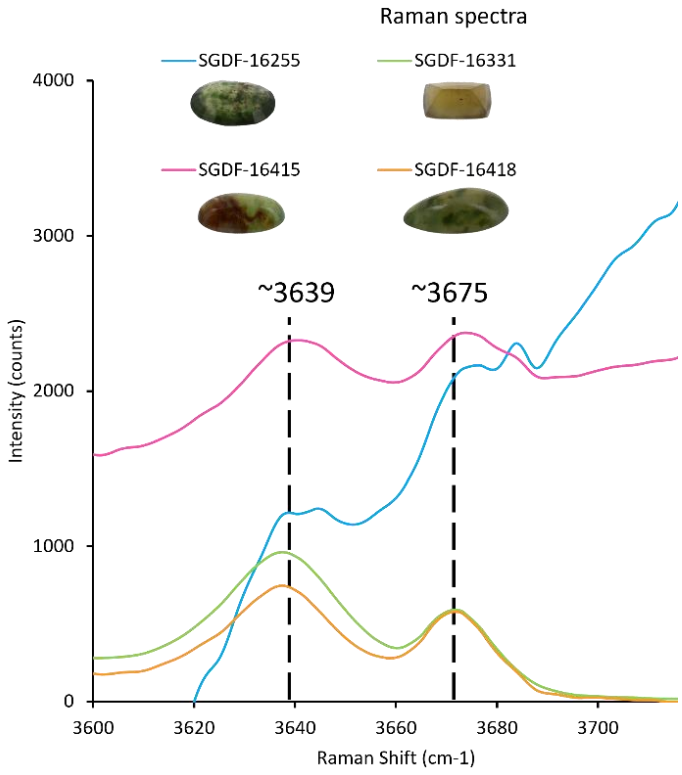

Figure 29: Two characteristic peaks of vesuvianite Raman spectra

Nevertheless, samples SGDF-16426, SGDF-16427, SGDF-16428 and SGDF-16429 have different Raman spectra from the others. In fact, these spectra have two bands at ~550 cm^{-1} and ~830 cm^{-1} which vesuvianite have not (represented by SGDF-16331 spectrum in the Figure 30). Concerning these bands, SGDF-16429 peak is largely higher (like six as much) than this of the three others. Then, another peak is remarkable at ~880 cm^{-1}. This is a very intense and thin band and once again this of SGDF-16429 is more intense than others. Nonetheless, vesuvianite spectra, represented by the red colour, has also this peak but smaller and wider.

Then, SGDF-16429 denotes the three others because SGDF-16426, SGDF-16427 and SGDF-16428 have some bands in common with vesuvianite as ~640 cm^{-1} or ~935 cm^{-1}. This at ~640 cm^{-1} is less wide and higher than this at ~935 cm^{-1}. Nevertheless, spectra highlight the fact that ~640 cm^{-1} peak exist in these three samples but with a lower intensity than vesuvianite sample SGDF-16331.

Finally, these four samples were identified as grossular. Remember that SGDF-16426, SGDF-16427 and SGDF-16428 were characterized as vesuvianite by IR-spectrometry but may be transitional samples between grossular and vesuvianite in view of their spectra. This hypothesis is supported by the presence of Raman bands similar to vesuvianite in SGDF-16426, SGDF-16427 and SGDF-16428 spectra and not visible in SGDF-16429 spectrum which was identified as grossular by the two methods.

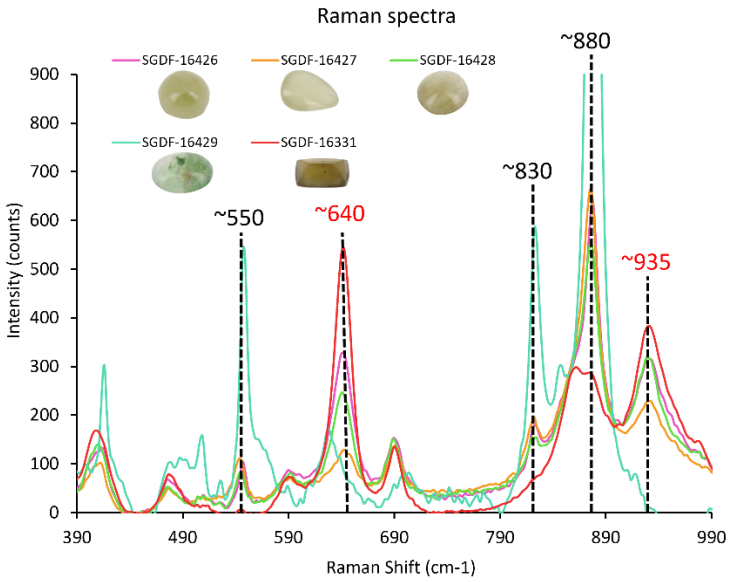

Figure 30: Grossular and transitional samples Raman spectra

- ## Others interpretations

Vesuvianite spectra can give us much information concerning atomic bonds in the crystal structure. In fact, according to Galuskin et al 2007, ~3635 cm^{-1} (~3639 cm^{-1}) band may correspond to Al (Y3) – Al (Y2) – OH liaisons. Also, ~3675 cm^{-1} peak shows Mg (Y3) – Al(Y2) – OH liaisons. However, these peaks ~3600 cm^{-1} may also correspond to structural water.

Additionally, Raman spectra can highlight the crystallization temperature of vesuvianite as we have seen in the IR absorbance part.

According to Galuskin et al 2007, crystallization temperatures can be deduced from the presence of some peaks in Raman spectra. In fact, a very high peak

located at ~3567 cm^{-1} associated with another one smaller at ~3635 cm^{-1} reflected high temperature vesuvianite. The big band at ~3567 cm^{-1} is absent on the spectra so our vesuvianite are not high temperatures. At the contrary, and in accordance with Galuskin et al 2007, vesuvianite peaks are present at ~3635 cm^{-1} and at ~3675 cm^{-1} that would mean we have low temperature vesuvianite. The majority of our 23 vesuvianite samples show a ~3635 cm^{-1} peak higher than the one at ~3675 cm^{-1}, meaning low vesuvianite corresponds Figure 29. We can see that SGDF-16255 and SGDF-16415 have not this characteristic even if these two bands are present. This is another arcticle, Butek 2024, which can help us to identified these samples as low temperature vesuvianite. In fact, it claims that low temperature vesuvianite have others specific bands at ~409cm^{-1}, ~643cm^{-1}, ~862cm^{-1} and ~930cm^{-1}. All these peaks can be found on vesuvianite IR spectra, that confirm our vesuvianite as low temperature. This hypothesis is also verified by Paluszkiewicz & Zabinski 2004, who show that low temperature vesuvianite has a more intense band at ~635 cm^{-1} (~640 cm^{-1} here) than ~695 cm^{-1} (~690 cm^{-1} in our case).

Finally, our Raman analyses combined with the bibliography, show our 23 samples of vesuvianite as low temperature vesuvianite. This result confirms the one of IR absorbance.

Another information about our vesuvianite samples come out of the fact that they are low temperature. In fact, according to Lu et al 2020 and Elmi et al 2011, low temperature vesuvianite would correspond to a P4/n space group. It corresponds to a four axes symmetry associated with a sliding mirror in the crystallin structure.

2) Chemical analyses

a) Vesuvianite chemical formulas

With the aim to analyse the chemical composition of our samples by elements quantification, a new method, specific to vesuvianite has been created. EDXRF is commonly depicted as a semi-quantitavie method. However, our results on vesuvianite, grossular and intergrown vesuvianite-grossular samples demonstrated a quite accurate quantification of major component. The new quantification method allows to quantify elements developed in the introduction. In addition of these elements, it was interesting trying to quantify REE in the samples because they are witness of the setting up of vesuvianite (Zhang et al 2022). Unfortunately, their trace concentrations are too low to be detected by EDXRF analyses. Quantifications was done in oxides weights since standards used to calibrate

Oxides	Mean values (%ox)	Ranges (%ox)	SGDF-16429 mean values (%ox)	SGDF-16426 mean values (%ox)
Na_2O	**BDL**	**BDL**	**BDL**	**BDL**
MgO	1,84 ± 0,04	0,818 - 2,521	0,97 ± 0,04	1,43 ± 0,04
Al_2O_3	16,45 ± 0,04	15,145 - 18,497	20,20 ± 0,05	16,59 ± 0,04
SiO_2	38,91 ± 0,05	36,443 - 42,934	39,92 ± 0,05	38,92 ± 0,05
SO_3	0,065 ± 0,003	0,0192 - 0,1692	0,076 ± 0,003	0,116 ± 0,003
Cl	0,36 ± 0,02	0,211 - 0,731	0,29 ± 0,02	0,31 ± 0,02
CaO	40,52 ± 0,03	35,465 - 43,824	37,26 ± 0,03	41,02 ± 0,03
Sc_2O_3	**BDL**	**BDL**	**BDL**	**BDL**
TiO_2	0,041 ± 0,001	0,00333 - 0,1214	0,108 ± 0,002	0,0053 ± 0,0008
Cr_2O_3	0,0529 ± 0,0007	0,000 - 0,2884	0,0589 ± 0,0009	0,0118 ± 0,0005
MnO	0,094 ± 0,001	0,05211 - 0,2348	0,0493 ± 0,0008	0,099 ± 0,001
Fe_2O_3	1,643 ± 0,005	0,8766 - 4,2334	1,024 ± 0,004	1,489 ± 0,004
CuO	0,0076 ± 0,0002	0,000 - 0,1132	0,0010 ± 0,0002	0,0004 ± 0,0002
ZnO	0,0027 ± 0,0002	0,00108 - 0,0076	0,0004 ± 0,0001	0,0046 ± 0,0002
Y_2O_3	**BDL**	**BDL**	**BDL**	**BDL**
PbO	0,0000 ± 0,0008	0,000 - 0,00023	0,0003 ± 0,0001	0,0003 ± 0,0001
Bi_2O_3	**BDL**	**BDL**	**BDL**	**BDL**
V_2O_5	0,0046 ± 0,0006	0,000 - 0,01113	0,0107 ± 0,0009	**BDL**
NiO	0,0107 ± 0,0004	0,000 - 0,05904	0,0137 ± 0,0004	0,0033 ± 0,0003

Table 2: Chemical quantification of different oxides, mean values and ranges

the method are mainly oxides. Results explain which elements occupy the crystalline structure and chemical formula of the mineral can be calculated. This formula can be compared with ideal formula of vesuvianite given by the IMA or Groat et al 1992.

Table 2) show data which are used to develop a mean chemical formula of our 23 vesuvianite given that there are not significant differences between samples chemistry. BDL means *Below Detection Limit*. All 27 sample's chemical formula were calculated (Annexe 5) with a normalization on 68 oxygen, and the results are shown on Annexe 6.

After calculations based on elements mean quantification, the mean chemical formulas of 23 vesuvianite samples is the following:

$$Ca_{19,008}\ (Al_{8,491}\ Fe_{0,541}\ Mg_{1,204}\ Mn_{0,035}\ Ti_{0,013}\ Cr_{0,018}\ Cu_{0,002}\ Zn_{0,001}\ V_{0,001}\ Ni_{0,004})\ Si_{17,038}\ O_{68.}$$

Then, we have:

$$X_{19,008}\ Y_{10,31}\ Z_{17,038}\ O_{68}$$

Remember that Groat et al 1992, gave $X_{19}\ Y_{13}\ Z_{18}\ O_{68}\ W_{10}$ as vesuvianite chemical formula. By the way, our X site has the perfect value comparing with literature. Also, our Z site, including Si, has also a correct value close to 18 atoms. We can see that Y site value is slightly weaker than the one of Groat et al 1992. This can be explained by the fact that the IMA associates Y site with vacancies. Remember that $Ca_{19}Fe^{3+}Al_4(Al_6Mg_2)(\square_4)\square[Si_2O_7]_4[(SiO_4)_{10}]O(OH)_9$ was the vesuvianite chemical formula given by the IMA. By the way these vacancies cannot by quantified with chemistry analyses but only deducted. Vacancies are possibly the reason why our Y site has a weaker value than expected (T sites for vacancies).

Then, analyses reveal presence of some anions which are in anionic site as W ($X_{19}\ Y_{13}\ Z_{18}\ O_{68}\ W_{10}$) in the formula given by Groat et al 1992. These anions are chlorine and sulphur. Their mean values in the 23 samples are respectively 0,36 % ± 0,02 and 0,065 % ± 0,003. As we said, these anions can be as substituent components in the crystalline structure but may also come from fluid inclusions in the structure. In fact, our vesuvianite are cryptocrystalline materials, so, many cracks are present between sites and can be filled by fluids. Chlorine and sulphur are often present in hydrothermal fluid at the roots of mineral setting up.

Besides, even if the mean chemical formula highlights 13 various elements in our samples, some vesuvianite have weak differences. These variations concern the presence or not of Cr, Cu, Zn, V and Ni because every sample has Ca, Al, Fe, Mg, Mn and Ti in close quantities. Nevertheless, we can quote one sample which differs by these major elements. In fact, SGDF-16331 has less calcium and more iron and aluminium than others 22 vesuvianite. Its chemical formula is the following: $X_{13,978}\ Y_{15,612}\ Z_{15,399}\ O_{68}$

$$Ca_{13,978}\ (Al_{13,655}\ Fe_{1,400}\ Mg_{0,514}\ Mn_{0,035}\ Ti_{0,004}\ Zn_{0,001}\ V_{0,001})\ Si_{15,396}\ O_{68}$$

This formula highlights differences which can be found in vesuvianite chemistry quantification. In fact, even if this sample was identified as vesuvianite by the IR and Raman analyses, its chemical formula is not completely similar to the ideal formula given by the literature.

b) Vesuvianite substitutions

Chemical analyses of vesuvianite samples have allowed to highlight the substitutions present in the structure. In introduction, plausible substitutions were quoted but chemical analyses allow to reject some. Indeed, due to the presence of Al, Mg, Fe, Ti and Mn in our results, the following substitution reactions can be accepted and probably happen in the structure:

- $Mg^{2+} \leftrightarrow Fe^{2+}$
- $Fe^{3+} \leftrightarrow Al^{3+}$
- $Al^{3+} \leftrightarrow Ti^{4+}$
- $Mg^{2+} \leftrightarrow Al^{3+}$
- $Mg^{2+} + Ti^{4+} \leftrightarrow 2Al^{3+}$ (in Y3 sites)
- $Mg^{2+}(+Fe^{2+}) + OH^{-} \leftrightarrow Al^{3+}(+Fe^{3+}) + O^{2-}$

However, light elements as bore or REE as lanthanide could not be quantified by our method. So, we cannot conclude about the presence or the absence of these elements. Nevertheless, it is sure that substitution reaction with sodium does not happen because our chemical result did not quantify any sodium in our samples.

c) Vesuvianite nominations

In the introduction, we have seen that it exists different vesuvianite species in vesuvianite group. After

chemical analyses we can make some conclusions about that. Firstly, we could not quantify bore and Fluor so we do not know if our samples are wiluite or fluorvesuvianite. However, we did not quantify so much copper in our results so our samples cannot be identified as cyprine. Also, according to Galuskin et al 2007, a mangavesuvianite need to have more than 0,5 Mn per formula to have this name. We have only 0.035 atoms per formula in our case so our samples are not mangavesuvianite.

d) Others samples results

Table 2 shows SGDF-16429 grossular mean values and SGDF-16426 as example of transitional sample between vesuvianite and grossular. SGDF-16426 is representative of SGDF-16427 and SGDF-16428 results. For the grossular and after calculations, we obtain the following chemical formula: $Ca_{3,021}Al_{1,802}Si_{3,021}O_{12}$.

The general formula of grossular given by the IMA (www.mindat.org/min-1755.html) is $Ca_3Al_2(SiO_4)_3$ that is to say $Ca_3Al_2Si_3O_{12}$. By the way this analyse confirm one time again the identity of SGDF-16429 as grossular in view of the very reliable results.

To continue, the specificity of transitional samples as SGDF-16426 is that the two formulas (vesuvianite and grossular) suit. For this sample, vesuvianite formula gives:

$Ca_{19,244}(Al_{8,563}Fe_{0,491}Mg_{0,932}Mn_{0,037}Ti_{0,002}Cr_{0,004}Zn_{0,001}Ni_{0,001})Si_{17,040}O_{68}$

That is to say, $X_{19,244}Y_{10,031}Z_{17,040}O_{68}$. This chemical formula is very close to others vesuvianite formulas.

Also, grossular formula for SGDF-16426 gives $Ca_{3,396}Al_{1,511}Si_{3,007}O_{12}$. This result suits also quite well for grossular identification.

Thereby, chemical analyses, demonstrate the double identity of our transitional samples. In fact, the two chemical formulas of vesuvianite and grossular suits, that reinforces IR and Raman results seen previously. As the Figure 31 shows, grossular and vesuvianite have similar global composition that which does not make surprising these transitional samples.

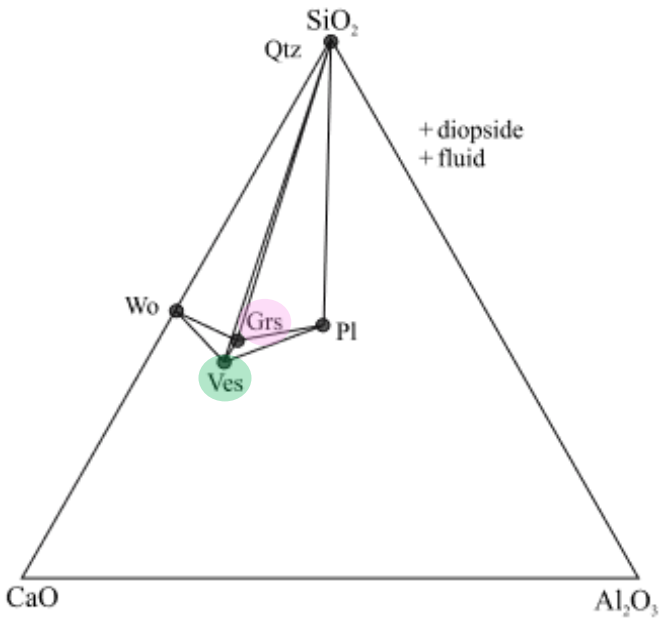

Figure 31: Diagram showing the close chemistry between vesuvianite and grossular (from Patel 2007 and modified by L. JOUGLA)

E) Colour analyses

1) UV-Vis-NIR spectroscopy

a) Raw spectra

UV-VIS-NIR spectroscopy is used with our 27 samples to analyse which colour of the visible spectrum reflects every cabochon. Macroscopically, samples have a diversity of colour from the pale yellow to dark green with brown variations. In fact, it is interesting to record UV spectra to highlight transmission windows of every sample. We analyse six cabochons with various appearances to show the differences between our samples.

The first sample (SGDF-16331) is described as brown cabochon in the Table 1. There are two transmission windows, the smallest at ~490nm in the blue domain and one bigger from the green-yellow to the red area. Human eye is less sensible to red colour and there is an absorption continuum toward UV wavelengths these are the reasons why this sample SGDF-16331 appears with a greenish-brown colour (Figure 32).

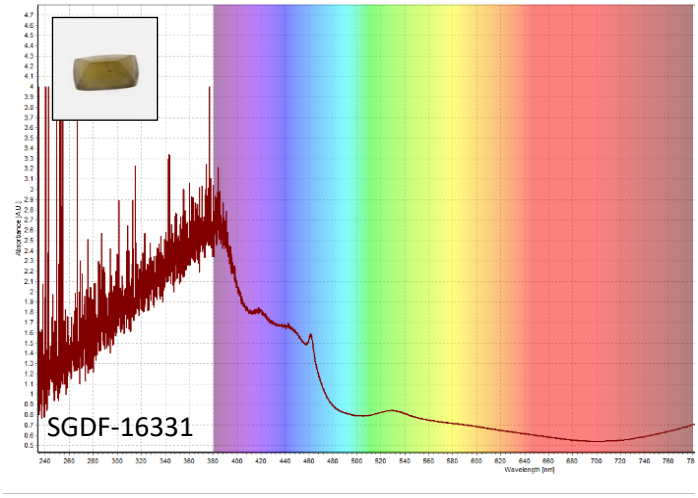

Figure 32: SGDF-16331 UV-Vis-NIR spectrum

SGDF-16383 sample appears, macroscopically, yellow-brown. On this UV-spectrum, a strong band is visible in the blue-violet domain with a maximum at ~430nm. This band precedes a large transmission window which reaches its maximum of transmission in the red area. Spectrum is mainly dominated by an absorption continuum toward the UV. Then, this is the similar reasons as SGDF-16331, why the sample SGDF-16383 appears yellow-brown or orange (Figure 33).

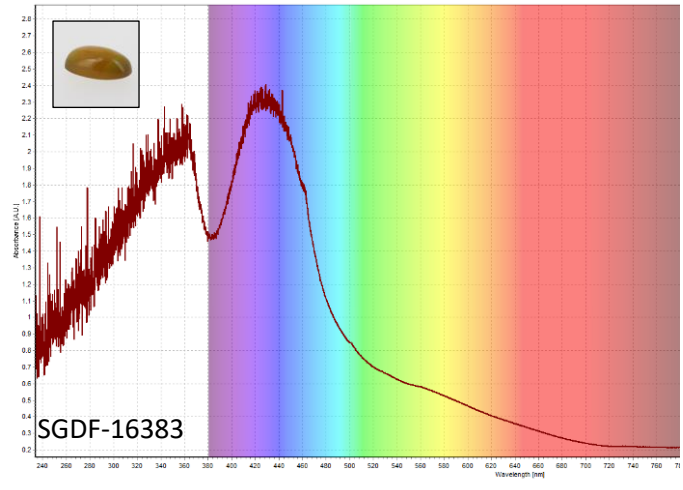

Figure 33: SGDF-16383 UV-Vis-NIR spectrum

The next cabochon, SGDF-16416 has a pale green colour with yellow hues. Its spectrum denotes the first because of the two small transmission windows in the green and yellow separated by a small band around 530 nm. Another decrease of the spectrum is present in the violet area at ~410nm but not strong enough to give this colour to the sample. Furthermore, the absorption continuum toward the UV is always present on this spectrum (Figure 34).

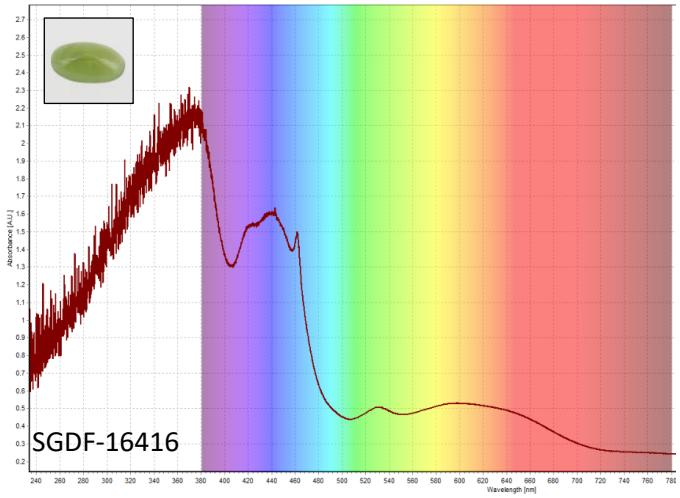

Figure 34: SGDF-16416 UV-Vis-NIR spectrum

The next sample, SGDF-16427 is the lighter of selected cabochons. It appears very light and a little green. This spectrum is very interesting because it highlights a much less intense band between ~420nm and ~460nm. The rest of the spectrum is very similar to the first sample SGDF-16331. The transmission window in the green area is just a little deeper than SGDF-16331. It may explain the green hues and the clearest colour of this sample more than the first one (Figure 35).

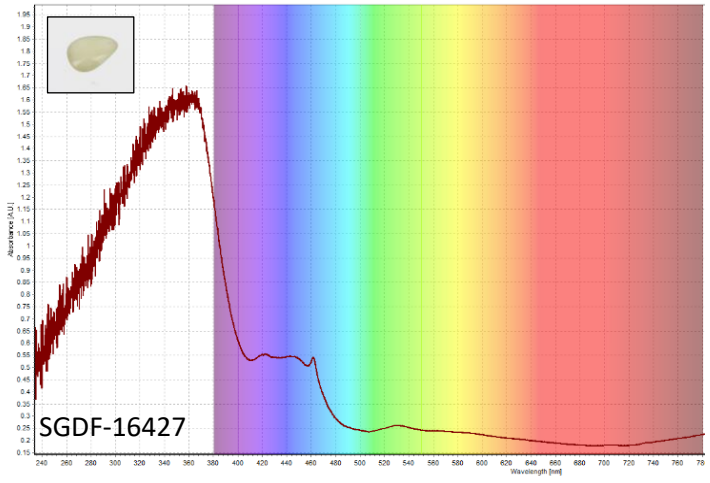

Figure 35: SGDF-16427 UV-Vis-NIR spectrum

SGDF-16429 is a very recognizable sample thank to its green-white bicolour aspect. The spectrum shows two pleasant bands at ~430nm and ~600nm separating three transmission windows at ~390nm, ~520nm and ~710nm. One more time the one in the violet area is too small to give the colour to the sample and the one in the red is not adapted for human eyes. This is the reason why SGDF-16429 has a green-white aspect macroscopically (Figure 36).

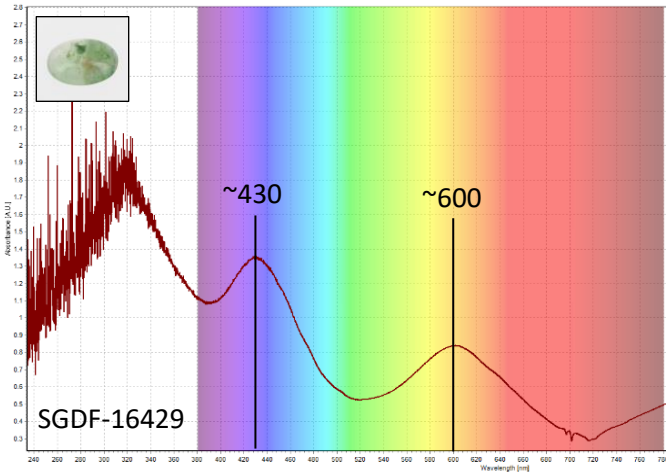

Figure 36: SGDF-16429 UV-Vis-NIR spectrum

The last sample has one of the darkest appearances. SGDF-16433 spectrum points out a clear transmission window in the blue-green area, this is the most indicative of the spectra described earlier. This window is surrounded by two bands as the one in green-yellow-red area which is very large. Therefore, the dark green colour of SGDF-16433 is justified by this transmission window at ~510nm (Figure 37).

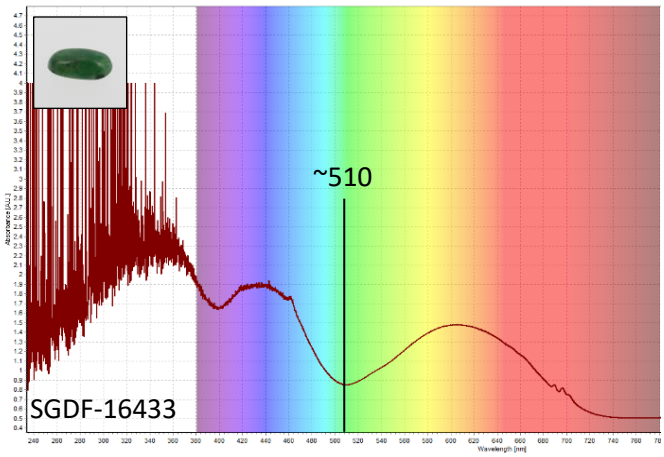

Figure 37: SGDF-16433 UV-Vis-NIR spectrum

b) UV-Visible spectroscopy taking thickness into account.

Absorption spectra can be analysed directly (precedent part) but are righter when optical path length is taken into account. In fact, with OMNIC software we can normalize spectra by the thickness of the sample and, therefore all of our spectra are more representative. With this calculate, ordinate become absorptivity. In fact, according **Beer Lambert** law, we have (Emmett et al 2023):

$$\boldsymbol{A = \varepsilon c l}$$

$\boldsymbol{A} = absorbance, \boldsymbol{\varepsilon} = molar\ absorptivity\ (L.mol^{-1}.cm^{-1}), \boldsymbol{c} = molar\ concentration\ (mol.L^{-1}), \boldsymbol{l} = path\ lenght\ (cm)$

And $\frac{\boldsymbol{A}}{\boldsymbol{l}} = \boldsymbol{\varepsilon c}$

Where $\boldsymbol{\varepsilon c}$ is the absorptivity because our samples are solids, so they have not molar concentration.

The superposition of our normalized spectra highlights absorption and transmission differences between our samples (Figure 38). SGDF-16433 denotes the others because of its large absorption bands at ~440nm and ~620nm. A smaller band and a very weak band are present respectively in SGDF-16429 and SGDF-16416 spectrum at ~620nm. According to Lu et al, 2020; these absorption bands around 600nm may correspond to the charges transfers between Fe^{2+} to Fe^{3+}. Also, ~620nm and ~410nm -~460nm transitions may correspond to Cr^{3+} in octahedral sites (Lu et al, 2020). Besides, vanadium band can also be present at ~600nm. By the way, this large band can correspond to an addition of two or more smaller bands. The band between 410nm and 460nm can be seen in every sample but with a less intensity in SGDF-16427 spectrum.

Chrome is a strong chromophore which may be responsible of the green colour and iron of the green-yellow sites. It is the reason why these absorption band appears only in the green samples (Lu et al, 2020). The peak between 410nm and 460nm may simultaneously correspond to Mn^{3+}. Then, we can raise a fine peak at ~460nm on four of our spectra. In fact, SGDF-16433, SGDF-16427, SGDF-16416 and SGDF-16331 have this peak which may correspond to Fe^{3+} in octahedral sites (Y1 or Y3) (Lu et al 2020).

Furthermore, weak increases in spectra can be raised. SGDF-16331, SGDF-16416 and SGDF-16427 have a small peak at ~530nm which may reflect effects of Mn^{3+}. Also, SGDF-16331 and SGDF-16429 spectra have a small and large band around ~850nm that can be find again but to a lesser extend in SGDF-16427 spectrum. This weak increase may also correspond to the charges transfers between Fe^{2+} to Fe^{3+} (Lu et al, 2020).

Ultimately, it is possible to say that our samples cover a wide range of colours from white-green to dark

green passing by brown, like the six samples studied in this part.

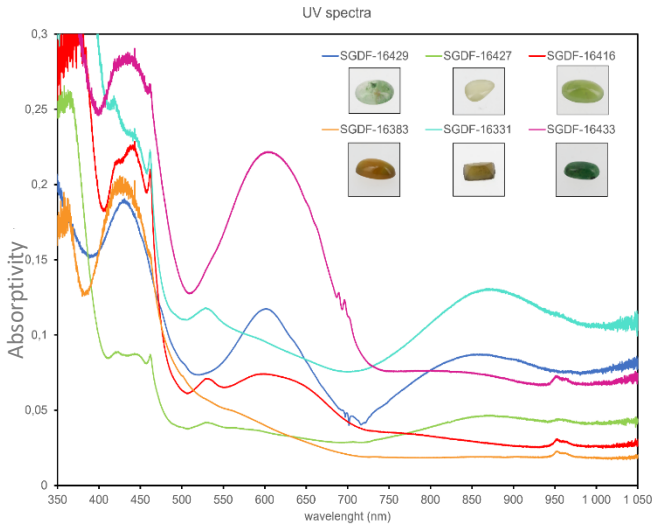

Figure 38: UV-Vis-NIR spectra of vesuvianite, grossular and transitional samples

c) Parallel chemical and UV results for vesuvianite

We can make a parallel between our chemical results seen previously and these UV spectra. For instance, if our interpretations are good SGDF-16433 should have more chromium, vanadium an iron than SGDF-16416, because the apparent maximum of absorptivity ~600nm of SGDF-16433 is higher than SGDF-16416. The chemical results show 0.08598 % of chromium in SGDF-16433 against 0.00523 % in SGDF-16416. Then, SGDF-16433 has 0.00574 % of vanadium against 0.00179% in SGDF-16416. Finally, SGDF-16433 has 1.4010 % of iron and SGDF-16416 has 2.1717 %. In conclusion, ~600nm band may actually correspond to chromium or vanadium but it would seem that iron does not correspond to this band because SGDF-16416 has more iron than SGDF-16433. Maybe a small band of iron can be present here but it is surpassed by the importance of chromium and vanadium band there.

It is possible to make the same reasoning for manganese and the apparent maximum of absorptivity at ~440nm. This peak may also highlight the presence of Cr. For SGDF-16433, the chemical quantification of Mn is 0.05221 % against 0.06658 % for SGDF-16416. We should expect the contrary in view of the spectra but we have to raise that an absorption continuum is present in the Figure 38. In fact, on high wavelengths, absorptivity does not reach the zero expected. This is because an absorption continuum lift spectra up on the graph. If we virtually supress this continuum, maybe SGDF-16416 spectrum will be higher than SGDF-16433 at ~440nm. This is the reason why it is not easy to correlate element quantification and absorptivity spectra for some elements as iron or manganese. In fact, the same analyse can be done with chemical values of iron of these two samples and the peak at ~850nm.

F) Description of the luminescence

It is interesting to look at our samples luminescence to see if they have all the same spectrum or not, especially to compare our vesuvianite.

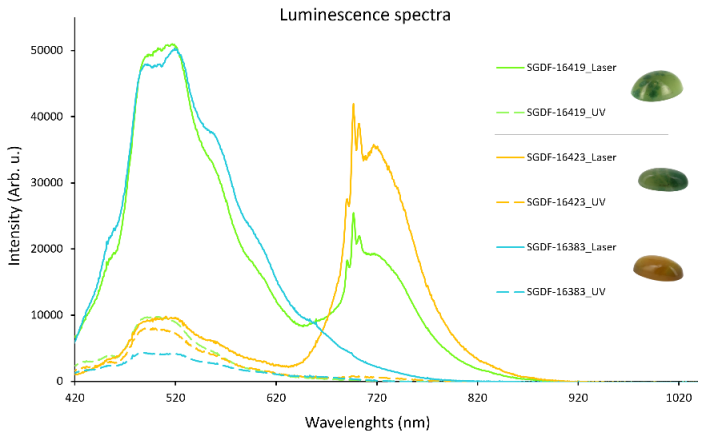

Figure 39: Three characteristic luminescence spectra of vesuvianite

Representative spectra of vesuvianite luminescence are shown in the Figure 39. These spectra represent the different luminescences seen in our samples. In fact, there are three discernible spectra. Vesuvianite luminescence spectrum can have a major and large band at ~720 nm characterized by thin triplets at ~700 nm. This spectrum is like the one of SGDF-16423 made with the laser. It is possible to see a small band at ~520 nm on the same spectrum. This luminescence peak is better shown on SGDF-16383_Laser spectrum. This band is a high and large peak and this is the unique on this spectrum. Otherwise, vesuvianite spectrum, as SGDF-16419_Laser spectrum can have these two peaks at ~720 nm and ~520 nm. It is possible to remark that the ~520 nm band is higher than the one at ~720 nm on this spectrum.

Also, all UV spectra highlight only a small band at ~520 nm. It highlights the fact that laser luminescence can capture better signals because it is concentrated on an only point.

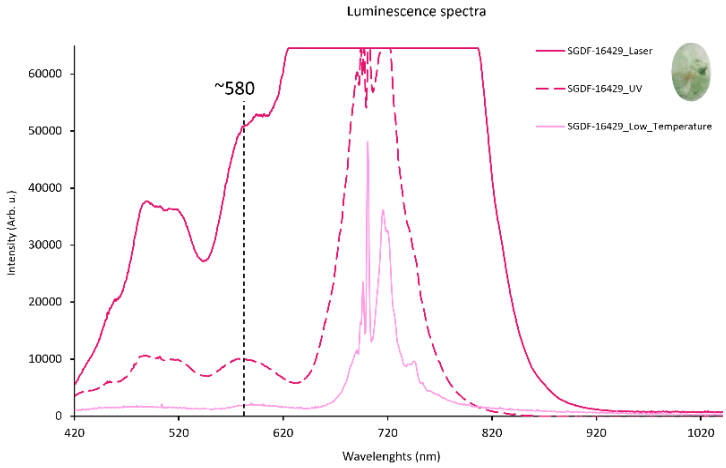

Figure 40: Grossular luminescence spectra

Furthermore, and one time again, SGDF-16429 sample is remarkable from others. In fact, the grossular has a different luminescence than vesuvianite. Spectra are shown on Figure 40. For this sample, low-temperature luminescence (with liquid nitrogen) was done to complete laser luminescence which was saturated. By the way, by combination of these two spectra, we can see precisely the different peaks of luminescence. We can recognize the same thin bands as vesuvianite at ~720 nm and the large one at ~520 nm. But there is one more peak in these spectra, shown by Laser and UV luminescence, this is the one at ~575 nm. This luminescence band is another characteristic which help us to distinguish grossular from vesuvianite.

Also, this difference between these two minerals can be done faster. In fact, by the eyes and thanks to UV light it is directly possible to make the difference because grossular has a pink luminescence and vesuvianite has one a blue/green. This fact is shown on Figure 41.

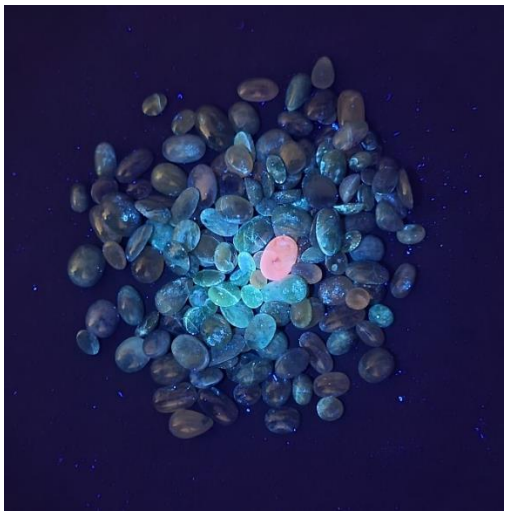

Figure 41: Group of vesuvianite with one grossular under UV light. The grossular appears in pink colour. (Photography by L. Jougla)

Besides, we can also analyse transitional samples luminescence spectra as the one of SGDF-16426, SGDF-16427 and SGGDF-16428. These spectra appear on Figure 42. Note that only UV luminescence spectrum was interpretable for SGDF-16428 sample. SGDF-16426 laser spectrum is similar as SGDF-16423 spectrum but difference by one more band at ~585 nm. This last one, as it was said previously, can be a witness of the grossular crystals which compose the sample with vesuvianite crystals. The same observation can be done with SGDF-16427 luminescence spectrum which is a similar spectrum as SGDF-16383 but also with the large band ~585 nm. Here again, we can remark the cryptocrystalline structure of a sample, combining grossular and vesuvianite crystals. These two bands are discernible on SGDF-16428 UV luminescence spectrum as SGDF-16426 and SGDF-16427.

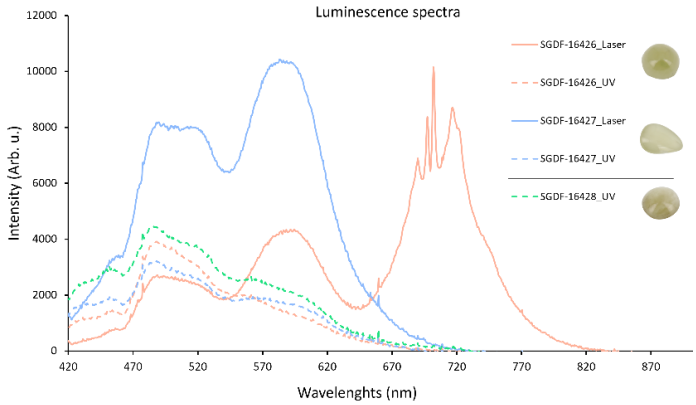

Figure 42: Luminescence spectra of transitional samples

G) Geological aspect

In this part, hypothesis of the setting up of our vesuvianite are made. Note that we have no information, no observation about the surrounding rocks where our materials were found. We just have the locality.

As we seen previously, according to Raman results, our vesuvianite samples are low temperature vesuvianite meaning a setting up at a temperature lower than 500°C, and mostly around 300°C (Paluszkiewicz & Zabinski 2004). According to them, high-temperature vesuvianite set up at 400°C- 800°C. Also, high vesuvianite corresponds to a skarn setting up environment (Patel 2007) and low vesuvianite appears in rodingites.

1) Vesuvianite setting up in a skarn environment, high temperatures and various cases

According to Jébrak et Marcoux 2008, skarn is a model of deposit which take place in recent magmatic arcs (~90 Ma), associated with small intrusions in a not much tectonized carbonate host. This model consists of three phases: one of thermometamorphism following by two episodes of metasomatism, one prograde and another retrograde. The episode of **metamorphism** is linked with an intrusion and a host dehydration. During this state, limestones are replaced by marble. Then, the **first stage of metasomatism**, at ~600-500°C, is associated with a supply of iron, manganese and aluminium bring by magmatic fluids released by the pluton. High temperature vesuvianite appears during this stage at the same time of others silicates. The following step is a **retrograde metasomatism** stage at a temperature around ~300-450°C. During this phase, hydrated minerals and sulphurs appear. A water influx causes the partial hydrolyse of minerals from the prograde step and the intrusion. This is the reason why, hydrated minerals as amphibole appear during this phase. The nature of these retrograde minerals depends of oxidation and sulphuration stages of hydrothermal fluids. It can be the reason why, Ghosh 2022, observed vesuvianite from this step.

In fact, Ghosh 2022, developed retrograde vesuvianite formation in his article, illustrated with the following schema (Figure 43).

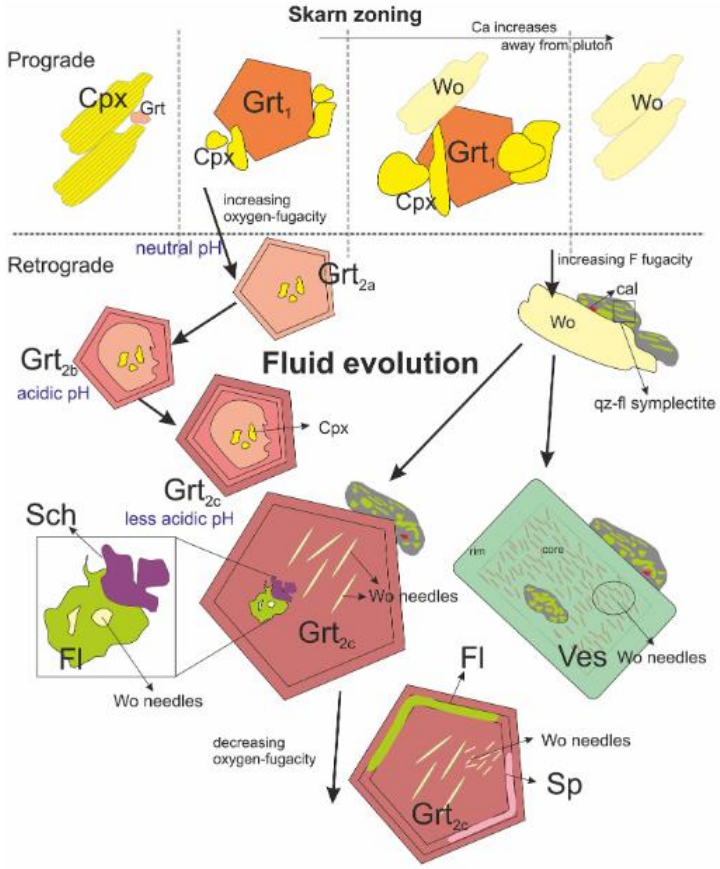

Figure 43: Prograde and retrograde mineral formation. Vesuvianite sets up during the retrograde stage (from Ghosh 2022)

He characterized its vesuvianite from this stage because he observed quartz and calcite symplectites in inclusions in vesuvianite. These symplectites would appear at the retrograde step leading retrograde vesuvianite, by the inclusion Principe. By the way, vesuvianite would be syn or post disappearance of wollastonite which is the origin of these symplectites. Gosh 2022 developed the chemical reaction following to described vesuvianite formation:

$$wollastonite + grossular + diopside + fluorite \rightarrow quartz + vesuvianite + carbon\ dioxide$$

That is to say:

$$CaSiO_3 + 2Ca_3Al_2(SiO_4)_3 + 2CaMgSi_2O_6 + 2H_2O + CaF_2 \rightarrow Ca_{10}Mg_2Al_4Si_9O_{34}(OH,F)_4 + 2SiO_2 + CO_2$$

It is important to say that its vesuvianite have an Al-rich composition as ours. By the way, this detail can guide us on this setting up hypothesis track. Also, even if the retrograde stage temperature of vesuvianite setting

up corresponds to our vesuvianite temperature, we did not observe neither quartz nor calcite crystallisations in our samples, that contradicts a little this hypothesis of setting up.

2) Low temperature vesuvianite, rodingite hosts

a) Vesuvianite in rodingites

According to Galuskin et al 2007, $Ca_{19}Al_9Mg_2Fe_2Si_{18}O_{69}OH_9$ vesuvianite ($(X_{19}Y_{13}Z_{18}O_{69}OH_9)$) were formed at low temperature in rodingites. This chemical formula of vesuvianite is very close to the one calculated with our samples, which is simplified as $X_{19}Y_{10}Z_{17}O_{68}$. In fact, rodingite environments for the setting up of our sample appears very suitable.

Normand 2001, published the pressure-temperature diagram shown on Figure 44. On this one, we can see the equilibrium boundaries for rodingite mineral assemblage and the stability area of vesuvianite in beige. This coloured area shows clearly a vesuvianite stability for a setting up around and lower 300°C in rodingites.

b) Rodingite definition

Rodingites are rocks formed by calciferous metasomatism initiated by hydrothermal fluids passage (Butek 2022). Rodingitisation process is closely linked with serpentinization process. These processus can be synchronous (Butek 2022) or continuous. In fact, rodingitisation can be just post serpentinization because Normand 2001 defined rodingites as calciferous rocks formed by serpentinite and adjacent lithologies rich in Al and Si metasomatism. By the way, we need to know serpentinization process to well analyse rodingitisation apparition.

Serpentinization process takes place in mafic and ultramafic host, this is a metamorphic. Consequently, serpentinites (and rodingites) are observed in environment as ophiolites (Butek 2022). Ophiolites are Mg-Fe rich rocks composed by minerals as olivine or pyroxenes. For instance, they include dunites, harzburgites or gabbros. Ophiolites are fragments from the oceanic lithosphere exhumated thanks to subduction or obduction mechanisms. Rodingitisation is also characteristic of the oceanic floor. So, the host rocks of rodingites vary but is often gabbroic (Butek 2022). Furthermore, vesuvianite set up only in the most affected by rodingitisation rocks.

c) Fluids at the origin of rodingitisation

Fluids bring a lot of various elements for the metasomatism but Al and Ti quantity present in vesuvianite reflect the Ti and Al contents of the protolith because they are immobile (Butek 2022). The hydrothermal fluid influx has to be important to have a vesuvianite crystallization. In fact, the report Si/Ca need

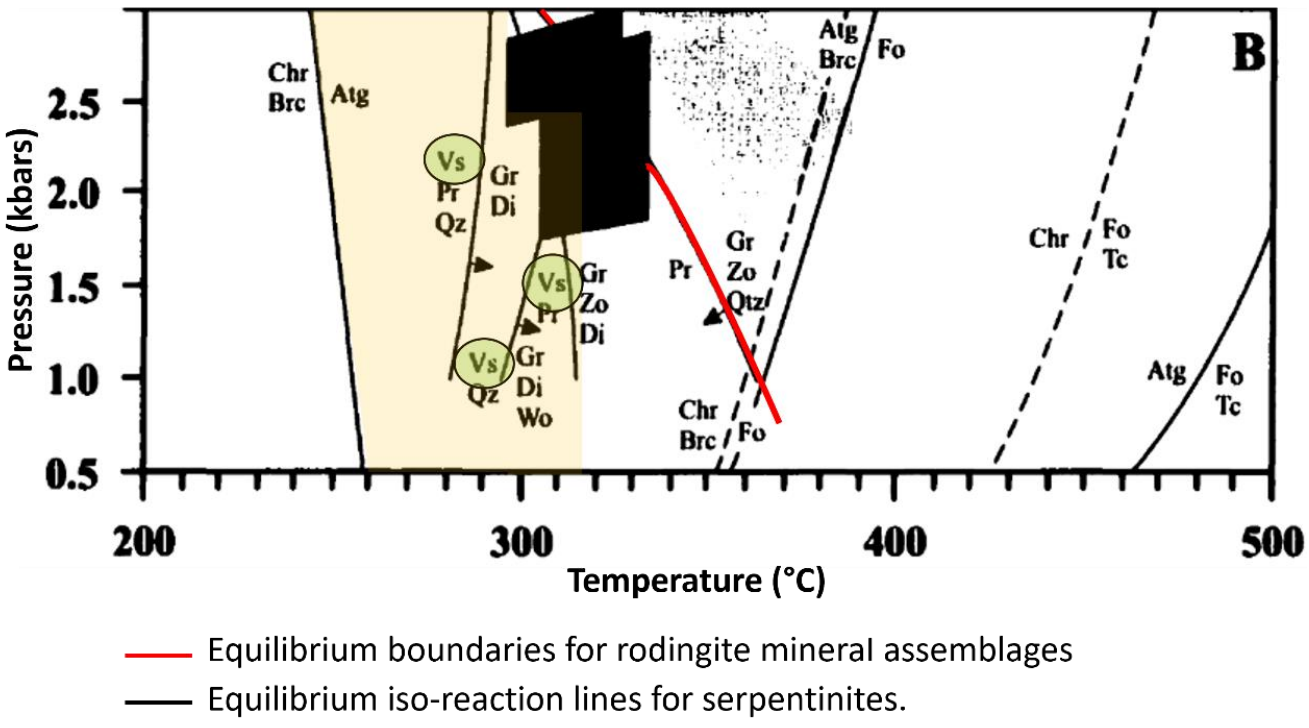

Figure 44: Pressure-temperature diagram in rodingites (from Normand 2001, modified by L. JOUGLA)

to decrease to have rodingites. Also, the diversity of rodingites in the world depends on the fluid quantity which percolate in rocks and not on the pressures-temperatures changes. This is linked by the fact that minerals present in rodingites are stable during a large range of pressures-temperatures. Besides, the hydrothermal fluids at the origin of the rodingites come from serpentinization process in ultramafic protoliths. These fluids have not Mg and S and have a weak content on Si. The provenance of the Ca may be the leaching of sedimentary rocks surroundings. The fluid is not composed of high contents of Ca because the weak content of Si is sufficient for the rodingitisation process. They have a high pH and a high reduction potential (Butek 2022). These chemical characteristics explain that changes in pH or oxido-reduction conditions can destabilize the fluid and result in mineral crystallizations in rodingites. Furthermore, CaO is very mobile during serpentinization, this is the reason why it can go in hydrothermal fluids to make Ca-rich metasomatism. The Figure 45 shows serpentinization and rodingitisation processus.

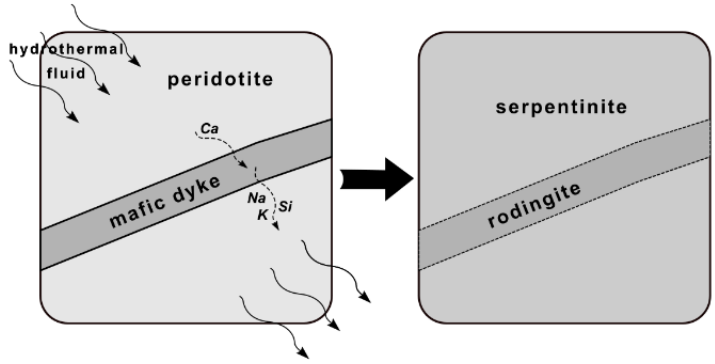

Figure 45: Schema explaining rodingitisation and serpentinisation processus (from Butek 2022)

d) Geological history and ophiolites areas in Afghanistan - Pakistan

We have seen that rodingitisation is linked with serpentinization and ophiolites, now it is important to replace all of that in the region geological history.

Afghanistan is one of the regions representing a witness of Indian and Eurasian plates. This collision at the origin of Himalaya chain is also linked with ophiolite exhumation in Central Asia and date of the early Paleogene (Jalil et al 2023).

Many ophiolites are present in the region as the Waziristan Ophiolite Complex (WOC) which is a suture zone between Indian and Pakistan plates. These Ophiolites was exhumated after an obduction episode as the Figure 46 shows.

Mafic and Ultramafic rocks undergoing serpentinization and rodingitisation are found in different part of Pakistan and Afghanistan as Kaboul, Jilal and Waziristan. These three ophiolites examples surround our vesuvianite samples' origins. This is the reason why, unknowing the real host of our vesuvianite, we can make the hypothesis that our localisation is composed of ophiolites too. These ophiolites are detailed on the Figure 47. We can see the mafic and ultramafic rocks and also the serpentinite presents in the Jijal Complex, to the East of Kunar Valley and in Kaboul ophiolites to the West.

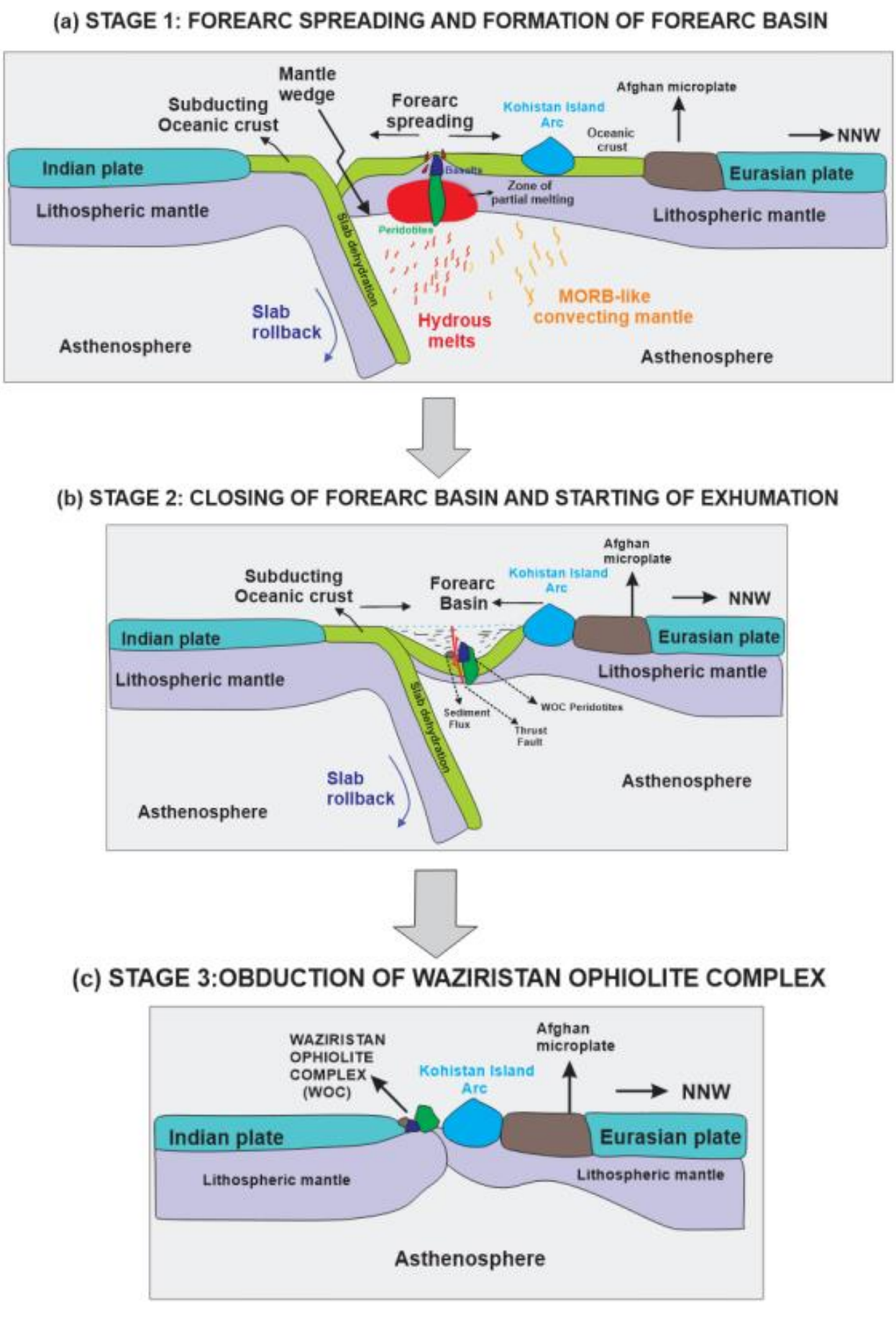

Figure 46: Geological history of the area and formation of the WOC (from Jalil et al 2023)

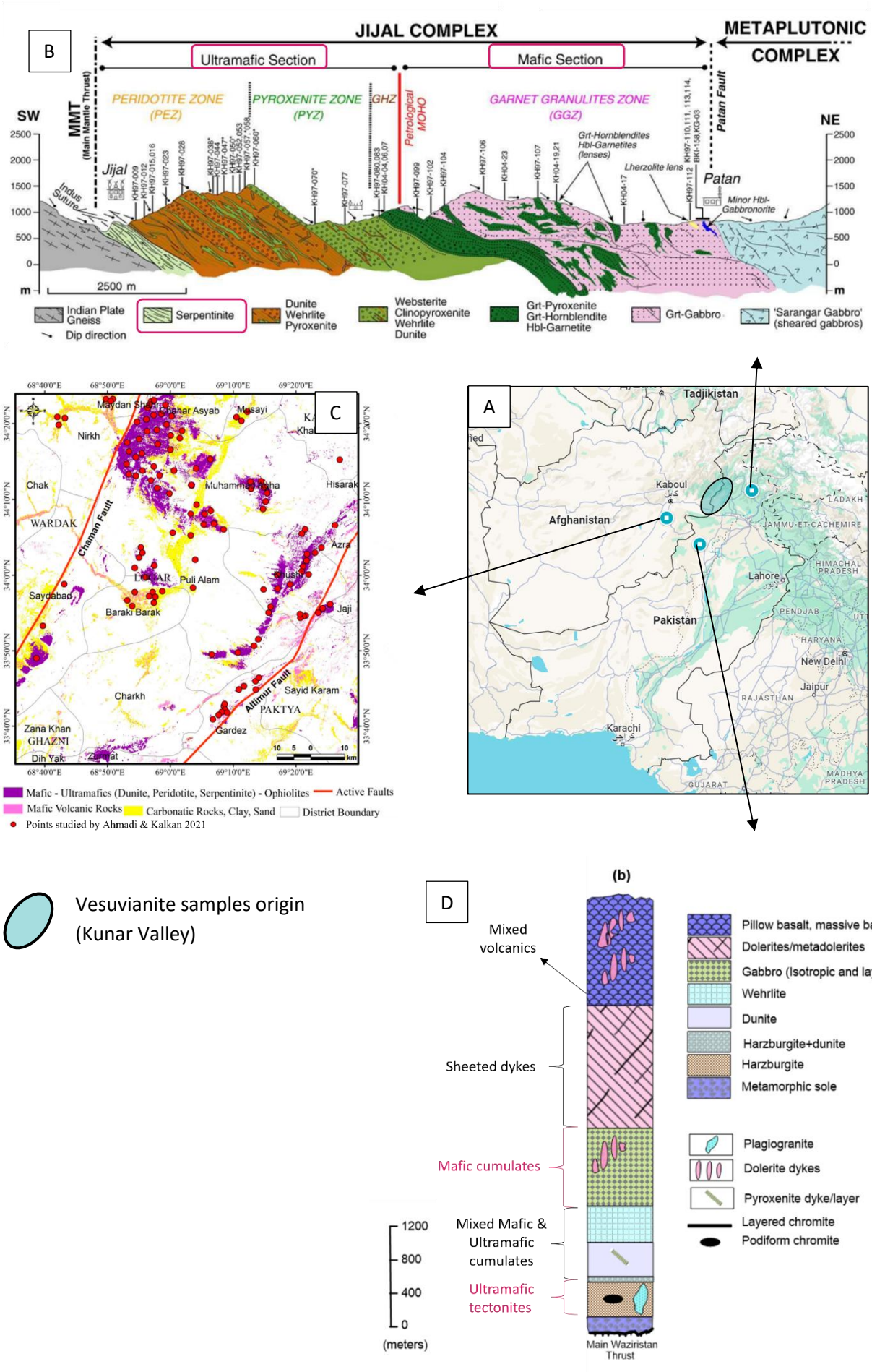

Figure 47: A: Afghanistan – Pakistan map with our vesuvianite origin and three ophiolite places around (adapted by L. Jougla from Google Maps), B: Cross-section of Jijal Mafic-Ultramafic complex in Kohistan Island Arc Complex (modified by L. Jougla from Dhuime et al 2007), C: Distribution of ophiolitic masses in Kabul ophiolites (modified by L. Jougla from Ahmadi & Kalkan 2021), ***D****: Waziristan Ophiolite Complex (modified by L. Jougla from Jalil et al*

e) Chemical reaction and relationship between vesuvianite and its inclusions

By the inclusion Principe, things contained in another thing is anterior as this latter. By the way, it is possible to say that inclusion in vesuvianite was formed before the crystallization of vesuvianite. Nevertheless, the polycrystalline feature of the materials facilitates fluids passage between layers or fissures. These fluids can crystallise and give inclusions in vesuvianite being posterior at our vesuvianite crystallisation. By the way, these two hypotheses are believable.

According to Butek 2022, vesuvianite grows instead of garnet solid solution. **Grossular**, with a chemical formula of $Ca_3Al_2(SiO_4)_3$ have been found in our vesuvianite samples. Grossular crystallise in rodingites or in contact or regionally metamorphosed area (www.mindat.org/min-1755.html). This information suits with all our hypothesis of the setting up of the materials studied. Some chemical reactions between vesuvianite and hydrogrossular explains what happened in our setting up environment. According to Butek 2022, hydrogrossular comes from reactions with calcium. This Ca would come from the leaching of Ca-rich rocks as sedimentary rocks transported by fluids. Chemical reactions with hydrogrossular and vesuvianite are the following:

- $hydrogrossular + chlorite + water \leftrightarrow vesuvianite \pm Ca, Na, Si\ minerals$
- $hydrogrossular + disthene + water \leftrightarrow vesuvianite + chlorite \pm Ca, Na, Si\ minerals$

Furthermore, when temperature increases, vesuvianite is less stable than hydrogrossular. The following chemical reactions happens (Normand 2001):

- $14\ prehnite + 3\ vesuvianite \leftrightarrow 5\ zoïcite + 6\ diopside + 23\ grossular + 25\ water$
- $prehnite + 5\ quartz + 2\ vesuvianite \leftrightarrow 4\ diopside + 12\ grossular + 10\ water$

Besides, **clinochlore** was found as inclusion in vesuvianite. This mineral, $Mg_5Al(AlSi_3O_{10})(OH)_8$ can have iron substitutions in its crystalline structure (www.mindat.org/min-1070.html). Clinochlore is frequent in ophiolite environments and also in areas metamorphized in greenschists facies. This facies is characteristic of the serpentinite rocks that is consistent with the approach we have. That highlights the fact that clinochlore was clearly present before the apparition of vesuvianite and that this one is posterior at this inclusion. So, clinochlore presence is one of the reasons why our vesuvianite have magnesium in their chemical formulas.

To continue, **covellite** inclusion, CuS, is present in vesuvianite materials. Covellite is present in areas which underwent metal-rich hydrothermalism, metamorphism and rarely volcanism (www.mindat.org/min-1144.html). Cu is a chalcophile element meaning a mantle provenance and a high affinity for sulphur. In fact, Cu might be in the host rocks of rodingitisation or might be bring by fluids with S.

Also, the **magnesiochromite**, $MgCr_2O_4$, found in vesuvianite samples are typical of ophiolites rocks (www.mindat.org/min-2493.html). This fact confirms one time again the ophiolitic host rocks of the rodingitisation process.

In addition, **amesite** inclusion of vesuvianite, $Mg_2Al(AlSiO_5)(OH)_4$, means a low-grade of metamorphism which coincides with serpentinization process. Amesite is often associated with magnetite and clinochlore (www.mindat.org/min-197.html) which can be present in mafic rocks as ophiolites as the view of their ferrous and magnesian features.

According to Jébrak & Marcoux 2008, **graphite** mineral crystallinity depends directly of the metamorphism degree. Metamorphism transforms organic residues, bitumen and sedimentary coal in graphitoid with a disrupted crystalline structure and after, in graphite better crystallised. Crystallised graphite appears with a temperature higher than 400°C. A moderate metamorphism gives an amorphous graphite as ones found in our vesuvianite. This temperature under 400°C suits with the setting up temperature found previously.

Finally, we can summarize the origins of the different elements present in the cryptocrystalline structure of vesuvianite. Elements as Fe, Mg or Al could come from the mafic and ultramafic rocks of ophiolites. Others like Ca and a little of Si could be a product of leached surrounding rocks by the metasomatic fluids which transported it until the deposit place. This deposit may depend on a lithological control because

rodingitisation is a process which take place on precise lithology, the one of mafic and ultramafic rocks. Also, as we said previously, these fluids have a basic pH and a high reduction potential (Butek 2022) meaning that a passage in oxidant or acid environment can destabilized these ones. Then, a chemical control of the deposit is also present in our case of setting up. At the end, it is possible to reject the physical control of the deposit because of the high stability of mineral in our range of pressures-temperatures (<500°C). Field observations could reject or accept a structural control of deposit but a priori, there is no reason to have a preferential deposit in fault or fractures for example.

IV - Discussions

Taking a step back, just little things might be interesting to improve in this study. Our results are statistically reliable because 27 samples were analysed for each experiment. Objectively, this is already a good number to make the results reliable even if more samples would be even better (but we need to have more time for the study).

Besides, it would be interesting if we had more precise information concerning the deposit. In fact, we only know the region where vesuvianite were extracted. We do not have any photography or observation of the deposit expression, no information about host rocks and surrounding rocks which constrains the geological aspect part to hypotheses.

Moreover, others methods would be interesting but many of them are destructive and the laboratory cannot use them. We can quote the Laser Induced Breakdown Spectroscopy (LIBS) which vaporises the material as a plasma and allows to quantify light elements as Li or B for example or Rare Earth Elements (REE). Laser Ablation-Inductively Coupled Plasma Mass Spectrometry (LA-ICP-MS) would also be helpful for the light element, but destructive too. Another method we can list is the XR-diffraction, on powder, which is a qualitative and quantitative method allowing to know the structure of the crystal system as stich parameters. Also, scanning electron microscope (SEM), which is a non-destructive method can give high resolution observations of samples, based on the interaction electron-material. This method could complete observations made by micrographies.

Conclusion

Through this study, characterisation of vesuvianite, grossular and combination of vesuvianite-grossular samples is done. Vesuvianite are very complex sorosilicates (www.mindat.org/min-4223.html) not much studied in research area even not studied at all as our vesuvianite from Kunar Valley in Afghanistan. Vesuvianite has a tetragonal system composed by five sites and the chemical formula can be written as: $X_{19}\,Y_{13}\,Z_{18}\,O_{68}\,W_{10}$. X sites are eight or nine coordinates, Y sites are five or six coordinates and Z sites are four coordinates. W sites constitute anionic sites (mono or di-anionic) with O^-, OH^- or F^-. International Mineralogical Association (IMA) gives the following chemical formula as an ideal formula: $Ca_{19}Fe^{3+}Al_4(Al_6Mg_2)(\square_4)\square[Si_2O_7]_4[(SiO_4)_{10}]O(OH)_9.I0$

27 samples from the set are chosen macroscopically and under the binocular loup for the study. These 27 samples have different characteristic as colours, inclusions or fractures interesting to identify. Gemological properties measures are firstly done highlighting a refraction index of 1.708 and various colours from the light greenish white to the vivid greenish yellow. The mean value of the specific mass of the sample is 3.374 ct what confirms vesuvianite identification. With a bright vitreous lustre, our vesuvianite have a good potential for jewellery. Besides micrographies and Raman analyses reveal various inclusions: greenish and automorphic grossular, colourful and automorphic clinochlore, black and automorphic inclusions as covellite or magnesiochromite and filamentous brownish inclusion identifies as amesite. Some black inclusions like stains reveal the presence of amorphous carbon that may be graphite.

Besides, IR and Raman analyses helped us to identify the materials. One sample is characterized as grossular (SGDF-16429) and three others as combinations of grossular and vesuvianite (SGDF-16426, SGDF-16427 and SGDF-16428). By the way 23 samples of the set are considered as vesuvianite. Chemical analyses by EDXRF quantify elements present in our 27 samples and allows to calculate chemical formulas for each sample and a mean formula reflecting the mean composition of the set. Finally, our mean chemical formula for vesuvianite is $Ca_{19,008}\,(Al_{8,491}\,Fe_{0,541}\,Mg_{1,204}\,Mn_{0,035}\,Ti_{0,013}\,Cr_{0,018}\,Cu_{0,002}\,Zn_{0,001}\,V_{0,001}\,Ni_{0,004})\,Si_{17,038}\,O_{68}$ that means $X_{19,008}\,Y_{10,31}\,Z_{17,038}\,O_{68}$ global formula. In

fact, X sites are occupied by Ca, Y sites by Al, Fe, Mg, Mn, Ti, Cr, Cu, Zn, V, Ni and Z sites by Si. By the way, some substitution reactions happen in vesuvianite crystals.

Grossular chemical formula is calculated as $Ca_{3,021}Al_{1,802}Si_{3,021}O_{12}$ and transitional samples as $Ca_{19,244}(Al_{8,563}Fe_{0,491}Mg_{0,932}Mn_{0,037}Ti_{0,002}Cr_{0,004}Zn_{0,001}Ni_{0,001})Si_{17,040}O_{68}$, that means $X_{19,244}Y_{10,031}Z_{17,040}O_{68}$ for vesuvianite and $Ca_{3,396}Al_{1,511}Si_{3,007}O_{12}$ for grossular, highlighting the cryptocrystallinity of these samples.

Furthermore, the colour analyses by UV-Vis-NIR spectra show green absorption (or absorptivity) by chromium or vanadium. Also, manganese and charge transfers between Fe^{2+} to Fe^{3+} are responsible of some absorption band in the blue and the red parts of sample spectra. Then, UV-luminescence can, one more time, highlight the difference between grossular and vesuvianite even macroscopically. In fact, grossular has a pink luminescence than vesuvianite has one blue/green. Also, by comparison with vesuvianite et grossular UV-luminescence spectra, ones of transitional samples are a combination of these two spectra showing the double characterisation with vesuvianite and grossular.

Also, Raman vesuvianite spectra give us information about the crystallisation temperature of these materials. In fact, we have low temperature vesuvianite at the view of our different peaks on spectra (Galuskin et al 2007, Butek 2024, Paluszkiewicz & Zabinski 2004). The crystallisation at low-temperature of our vesuvianite is characteristic of the rodingitisation process. Rodingites are rocks created by metasomatism, more precisely Ca-metasomatism, which takes place with serpentinization process (Butek 2022). By the way, rodingites are formed in mafic and ultramafic rocks as ophiolites. The region where our vesuvianite were extracted is probably rich in ophiolites because many surrounding rocks constitute ophiolites as Kabul (Afghanistan), Jilal (Kohistan) and Waziristan (WOC). These ophiolites are witnesses of the rich geological events which took place in this geographical area, as intra-oceanic subduction or peridotite formation and exhumation. In the end, relationship between inclusions, vesuvianite and its composition has been done with a geological point of view.

Finally, this study allowed me to browse a large field of geosciences and gemmology as crystallography, mineralogy, chemistry, calculates with chemical formulas or geological setting up of the deposit.

Bibliography

Abart, R., 1995. Phase equilibrium and stable isotope constraints on the formation of metasomatic garnet-vesuvianite veins (SW Adamello, N Italy). Contributions to Mineralogy and Petrology 122, 116–133. https://doi.org/10.1007/s004100050116

Ahmadi, H., Kalkan, K., 2021. Mapping of Ophiolitic Complex in Logar and Surrounding Areas (SE Afghanistan) With ASTER Data. J Indian Soc Remote Sens 49, 1271–1284. https://doi.org/10.1007/s12524-021-01319-4

Aksenov, S.M., Chukanov, N.V., Rusakov, V.S., Panikorovskii, T.L., Rastsvetaeva, R.K., Gainov, R.R., Vagizov, F.G., Lyssenko, K.A., Belakovskiy, D.I., 2016. Towards a revisitation of vesuvianite-group nomenclature: the crystal structure of Ti-rich vesuvianite from Alchuri, Shigar Valley. Acta Crystallogr B Struct Sci Cryst Eng Mater 72, 744–752. https://doi.org/10.1107/S2052520616010246

Butek, J., n.d. Les rodingites des Carpathes occidentales: minéralogie et géochimie.

Czaja, M., Lisiecki, R., Chrobak, A., Sitko, R., Mazurak, Z., 2018. The absorption- and luminescence spectra of Mn3+ in beryl and vesuvianite. Phys Chem Minerals 45, 475–488. https://doi.org/10.1007/s00269-017-0934-x

Dhuime, B., Bosch, D., Bodinier, J.-L., Garrido, C.J., Bruguier, O., Hussain, S.S., Dawood, H., 2007. Multistage evolution of the Jijal ultramafic–mafic complex (Kohistan, N Pakistan): Implications for building the roots of island arcs. Earth and Planetary Science Letters 261, 179–200. https://doi.org/10.1016/j.epsl.2007.06.026

Elmi, C., Brigatti, M.F., Pasquali, L., Montecchi, M., Laurora, A., Malferrari, D., Nannarone, S., 2011. High-temperature vesuvianite: crystal chemistry and surface considerations. Phys Chem Minerals 38, 459–468. https://doi.org/10.1007/s00269-011-0419-2

Emmett, J.L., Atikarnsakul, U., Stone-Sundberg, J., Sangsawong, S., 2023. Yellow Sapphire: Natural, Heat-Treated, Beryllium-Diffused, and Synthetic. G&G 59, 268–297.

https://doi.org/10.5741/GEMS.59.3.268

Ferrari, A.C. & Robertson, J. 2000. Interpretation of Raman spectra of disordered and amorphous carbon. *Physical Review B*, **61**(20), 14095–14107, https://doi.org/10.1103/PhysRevB.61.14095.

Fitzgerald, S., Rheingold A., Leavens P.B., 1986. Crystal strucrure of a non-P4/nnc vesuvianite from Asbestos, Quebec. *American Mineralogist*, Volume 71, pages 1483-148

Gaft, M., Reisfeld, R., & Panczer, G., 2015. Modern luminescence spectroscopy of minerals and materials. In *Modern Luminescence Spectroscopy of Minerals and Materials* (2nd ed.). Springer.

Galuskin, E., Janeczek, J., Kozanecki, M., Sitarz, M., Jastrzębski, W., Wrzalik, R., Stadnicka, K., 2007. Single-crystal Raman investigation of vesuvianite in the OH region. Vibrational Spectroscopy 44, 36–41. https://doi.org/10.1016/j.vibspec.2006.06.022

Ghosh, U., 2022. The retrograde evolution of F-rich skarns: Clues from major and trace element chemistry of garnet, scheelite, and vesuvianite from the Belka Pahar wollastonite deposit, India.

Groati, L.A., Hawthorne, F.C., Ercit, T.S., n.d. THE CHEMISTRY OF VESUVIANITE. THE CANADIAN MINERALOGIST.

Jalil, R., Alard, O., Schaefer, B., Ali, L., Sajid, M., Khedr, M.Z., Shah, M.T., Anjum, M.N., 2023. Geochemistry of Waziristan Ophiolite Complex, Pakistan: Implications for Petrogenesis and Tectonic Setting. Minerals 13, 311. https://doi.org/10.3390/min13030311

Jébrak, M., Marcoux, E., 2008. Géologie des ressources minérales. Ministère des ressources naturelles et de la faune, Québec.

Kobayashi, S., Kaneda, H., 2010. Rodingite with Ti- and Cr-rich vesuvianite from the Sartuohai chromium deposit, Xinjiang, China. Journal of Mineralogical and Petrological Sciences 105, 112–122. https://doi.org/10.2465/jmps.081224

Lu, Z., He, X., Lin, C., Liang, L., Jin, X., Guo, Q., 2020. Color and genesis of californite from Pakistan: insights from μ-XRF mapping, optical spectra and X-ray photoelectron spectroscopy. Sci Rep 10, 285. https://doi.org/10.1038/s41598-019-57186-0

Manutchehr-Danai M., 2005. Dictionary of gems and gemology. Springer Science & Business Media.

Medenbach, O., Sussieck-Fornefeld, C., 1982. Les minéraux. La nature en couleurs. FRANCE LOISIRS.

Mindat.org. Title [Amesite]. URL www.mindat.org/min-197.html (accessed 26/08/2024)

Mindat.org. Title [Clinochlore]. URL www.mindat.org/min-1070.html (accessed 26/08/2024)

Mindat.org. Title [Covellite]. URL www.mindat.org/min-1144.html (accessed 26/08/2024)

Mindat.org. Title [Grossular]. URL www.mindat.org/min-1755.html (accessed 26/08/2024)

Mindat.org. Title [Magnesiochromite]. URL www.mindat.org/min-2493.html (accessed 26/08/2024)

Mindat.org. Title [Vesuvianite]. URL www.mindat.org/min-4223.html (accessed 26/08/2024)

Paluszkiewicz, C., Żabiński, W., 2004. Vibrational spectroscopy as a tool for discrimination of high and low vesuvianite. Vibrational Spectroscopy 35, 77–80. https://doi.org/10.1016/j.vibspec.2003.11.021

Patel, S.C., 2007. Vesuvianite-wollastonite-grossular-bearing calc-silicate rock near Tatapani, Surguja district, Chhattisgarh. J Earth Syst Sci 116, 143–147. https://doi.org/10.1007/s12040-007-0014-6

Reisfeld, R., Gaft, M., Boulon, G., Panczer, C., Jørgensen, C.K., 1996. Laser-induced luminescence of rare-earth elements in natural fluor-apatites. Journal of Luminescence 69, 343–353. https://doi.org/10.1016/S0022-2313(96)00114-7

Smart, M.M., Moore, C.A., McMillen, C.D., Kolis, J.W., 2023. Hydrothermal Synthesis and Crystal Structure of Vesuvianite Compounds,

Ca19Al13Si18O71(OH)7 and Sr19Fe12Ge19O72(OH)6. Crystals 13, 1257. https://doi.org/10.3390/cryst13081257

Smith, E.M., Shirey, S.B., Wang, W., 2018. The Very Deep Origin of the World's Biggest Diamonds. G&G 53, 388–403. https://doi.org/10.5741/GEMS.53.4.388

Zhang, Y., Song, S., Hollings, P., Li, D., Shao, Y., Chen, H., Zhao, L., Kamo, S., Jin, T., Yuan, L., Liu, Q., Chen, S., 2022. In-situ U Pb geochronology of vesuvianite in skarn deposits. Chemical Geology 612, 121136. https://doi.org/10.1016/j.chemgeo.2022.121136

Annexes

Annexe 1: Gradation of colours of six samples (by L. Jougla)

Références	Masses in the air (ma)	Masses in the water (mw)	Specific masses = ma/(ma-mw)
SGDF-16420	8,562	6,032	3,384189723
SGDF-16429	19,823	14,26	3,563365091
SGDF-16255	4,904	3,458	3,39142462
SGDF-16430	14,695	10,337	3,371959615
SGDF-16423	17,999	12,612	3,341191758
SGDF-16415	11,123	7,786	3,333233443
SGDF-16431	17,86	12,518	3,34331711
SGDF-16433	14,567	10,162	3,30692395
SGDF-16428	13,877	9,888	3,478816746
SGDF-16413	9,776	6,842	3,331970007
SGDF-16424	10,288	7,201	3,332685455
SGDF-16426	5,476	3,862	3,392812887
SGDF-16383	64,531	45,227	3,342882304
SGDF-16432	10,201	7,151	3,344590164
SGDF-16421	19,491	13,815	3,433932347
SGDF-16302	9,173	6,462	3,38362228
SGDF-16414	30,409	21,352	3,357513525
SGDF-16331	8,376	5,93	3,424366312
SGDF-16419	12,813	8,99	3,351556369
SGDF-16422	11,276	7,903	3,343018085
SGDF-16425	4,4	3,095	3,37164751
SGDF-16417	8,861	6,218	3,352629588
SGDF-16418	10,613	7,444	3,349005996
SGDF-16317	16,115	11,312	3,35519467
SGDF-16427	8,708	6,14	3,390965732
SGDF-16272	4,257	3,001	3,38933121
SGDF-16416	16,709	11,716	3,346485079
		Mean value	3,374393762

Annexe 2: Specific mass calculates with masses in the air and in the water

Annexe 3: Lustre scale with other materials (by L. Jougla)

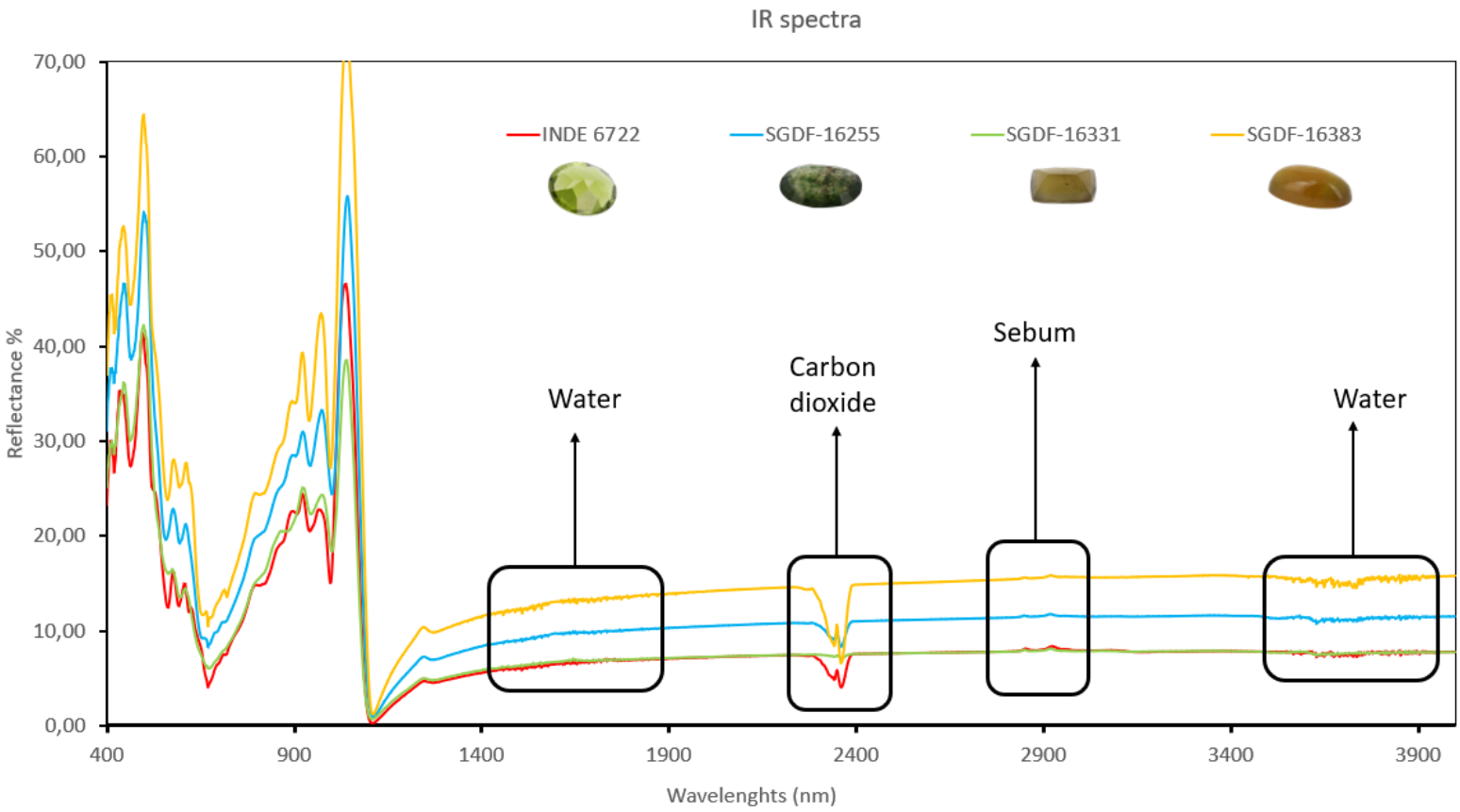

Annexe 4: IR spectra with water, carbon dioxide and sebum characteristic peaks

Results of the chemical analyses (normalized column)

SGDF-16383								
oxides	Chemical quantifications	Molar Masses	% Molar	% Molar on 100	Number of element	Number of oxygen	Oxygen on 68	Cations on 68 oxydes
Na2O	0	61,979	0	0	0	0	0	0
MgO	2,521	40,304	0,062549623	3,91406687	3,91406687	3,91406687	1,616359544	1,616359544
Al2O3	18,497	101,961	0,181412501	11,35195748	22,70391497	34,05587245	14,06376955	9,375846367
SiO2	40,355	60,084	0,671643033	42,02832285	42,02832285	84,0566457	34,71217177	17,35608589
SO3	0,0332	80,062	0,000414679	0,025948675	0,025948675	0,077846026	0,032147424	0,010715808
Cl	0,477	35,453	0,013454433	0,841916331	0,841916331	0	0	0,347679164
CaO	37,05	56,077	0,660698682	41,34347585	41,34347585	41,34347585	17,07327034	17,07327034
Sc2O3	0	137,909	0	0	0	0	0	0
TiO2	0,01734	79,965	0,000216845	0,013569152	0,013569152	0,027138303	0,011207079	0,005603539
Cr2O3	0	151,989	0	0	0	0	0	0
MnO	0,134	70,937	0,001889	0,118204913	0,118204913	0,118204913	0,048814097	0,048814097
Fe2O3	0,9039	159,687	0,005660448	0,354204741	0,708409482	1,062614223	0,438818931	0,292545954
CuO	0	79,545	0	0	0	0	0	0
ZnO	0,00576	81,379	7,07799E-05	0,004429082	0,004429082	0,004429082	0,001829041	0,001829041
Y2O3	0	225,809	0	0	0	0	0	0
PbO	0	223,199	0	0	0	0	0	0
Bi2O3	0	465,957	0	0	0	0	0	0
V2O5	0	181,879	0	0	0	0	0	0
NiO	0,00466	74,692	6,23895E-05	0,00390405	0,00390405	0,00390405	0,001612223	0,001612223
			1,598072413			164,6641975		

Sum of the column (Sum1)

Sum of the column (Sum2)

$$\%\ molar = \frac{chemical\ quantification}{Molar\ masses}$$

$$\%\ molar\ on\ 100 = \frac{\%\ molar\ * 100}{Sum1}$$

$$number\ of\ element = coeficient\ of\ the\ element\ in\ the\ oxide * \%\ molar\ on\ 100$$

$$number\ of\ element = coeficient\ of\ oxygen\ in\ the\ oxide * \%\ molar\ on\ 100$$

$$oxygen\ on\ 68 = \frac{number\ of\ oxygen\ * 68}{Sum2}$$

$$cations\ on\ 68 = \frac{number\ of\ element\ * 68}{Sum2}$$

Annexe 6: Chemical formulas calculated from chemical quantification by EDXRF

Samples	Chemical formulas	General formulas	
		Vesuvianite	Grossular
SGDF-16420	$Ca_{19,582}(Al_{8,351}Fe_{0,660}Mg_{1,098}Mn_{0,035}Ti_{0,002}Zn_{0,001}Ni_{0,001})Si_{16,841}O_{68}$	$X_{19,582}Y_{10,148}Z_{16,841}O_{68}$	
SGDF-16429	$Ca_{3,021}Al_{1,802}Si_{3,021}O_{12}$		$Ca_{3,021}Al_{1,802}Si_{3,021}O_{12}$
SGDF-16255	$Ca_{18,655}(Al_{8,503}Fe_{0,406}Mg_{1,141}Mn_{0,037}Ti_{0,026}Cr_{0,099}Cu_{0,018}Zn_{0,001}V_{0,003}Ni_{0,021})Si_{17,194}O_{68}$	$X_{18,655}Y_{10,255}Z_{17,194}O_{68}$	
SGDF-16430	$Ca_{19,481}(Al_{8,620}Fe_{0,540}Mg_{0,848}Mn_{0,027}Ti_{0,008}Cr_{0,003}V_{0,001})Si_{16,914}O_{68}$	$X_{19,481}Y_{10,047}Z_{16,914}O_{68}$	
SGDF-16423	$Ca_{19,884}(Al_{8,182}Fe_{0,438}Mg_{1,269}Mn_{0,027}Ti_{0,017}Cr_{0,004}Zn_{0,001}V_{0,002}Ni_{0,002})Si_{16,897}O_{68}$	$X_{19,884}Y_{9,942}Z_{16,897}O_{68}$	
SGDF-16415	$Ca_{16,157}(Al_{8,776}Fe_{0,359}Mg_{1,401}Mn_{0,085}Ti_{0,011}Cr_{0,011}Zn_{0,002}V_{0,002}Ni_{0,003})Si_{18,256}O_{68}$	$X_{16,157}Y_{10,65}Z_{18,256}O_{68}$	
SGDF-16431	$Ca_{19,361}(Al_{8,506}Fe_{0,656}Mg_{1,307}Mn_{0,024}Ti_{0,014}Cr_{0,001}V_{0,001}Ni_{0,003})Si_{16,745}O_{68}$	$X_{19,361}Y_{10,512}Z_{16,745}O_{68}$	
SGDF-16433	$Ca_{19,420}(Al_{8,220}Fe_{0,463}Mg_{1,554}Mn_{0,019}Ti_{0,010}Cr_{0,030}Zn_{0,001}V_{0,002}Ni_{0,005})Si_{16,914}O_{68}$	$X_{19,420}Y_{10,3}Z_{16,914}O_{68}$	
SGDF-16428	$Ca_{19,478}(Al_{9,283}Fe_{0,436}Mg_{0,232}Mn_{0,027}Ti_{0,016}Cr_{0,001}Ni_{0,002})Si_{16,792}O_{68}$ **or** $Ca_{3,437}Al_{1,638}Si_{2,963}O_{12}$	$X_{19,478}Y_{9,997}Z_{16,792}O_{68}$	$Ca_{3,437}Al_{1,638}Si_{2,963}O_{12}$
SGDF-16413	$Ca_{18,866}(Al_{8,525}Fe_{0,288}Mg_{1,412}Mn_{0,043}Ti_{0,003}Zn_{0,001})Si_{17,188}O_{68}$	$X_{18,866}Y_{10,272}Z_{17,188}O_{68}$	
SGDF-16424	$Ca_{20.049}$ $(Al_{8,088}Fe_{0,592}Mg_{1,452}Mn_{0,038}Ti_{0,040}Cr_{0,048}Zn_{0,001}V_{0,003}Ni_{0,003})Si_{16,614}O_{68}$	$X_{20.049}Y_{10.265}Z_{16.614}O_{68}$	
SGDF-16426	$Ca_{19,244}$ $(Al_{8,563}Fe_{0,491}Mg_{0,932}Mn_{0,037}Ti_{0,002}Cr_{0,004}Zn_{0,001}Ni_{0,001})Si_{17,040}O_{68}$ **or** $Ca_{3,396}Al_{1,511}Si_{3,007}O_{12}$	$X_{19,244}Y_{10,031}Z_{17,040}O_{68}$	$Ca_{3,396}Al_{1,511}Si_{3,007}O_{12}$
SGDF-16383	$Ca_{17,073}$ $(Al_{9,376}Fe_{0,293}Mg_{1,616}Mn_{0,049}Ti_{0,006}Zn_{0,002}Ni_{0,002})Si_{17,356}O_{68}$	$X_{17,073}Y_{11,344}Z_{17,356}O_{68}$	
SGDF-16432	$Ca_{19,805}(Al_{8,216}Fe_{0,710}Mg_{1,130}Mn_{0,025}Ti_{0,022}Cr_{0,024}V_{0,001}Ni_{0,002})Si_{16,753}O_{68}$	$X_{19,805}Y_{10,13}Z_{16,753}O_{68}$	
SGDF-16421	$Ca_{20,139}(Al_{8,212}Fe_{0,499}Mg_{1,210}Mn_{0,03}Ti_{0,007}Cr_{0,001}V_{0,001}Ni_{0,002})Si_{16,731}O_{68}$	$X_{20,139}Y_{9,962}Z_{16,731}O_{68}$	
SGDF-16302	$Ca_{20,954}(Al_{8,367}Fe_{0,450}Mg_{0,986}Mn_{0,038}Ti_{0,031}Cr_{0,067}Cu_{0,038}Zn_{0,001}V_{0,003}Ni_{0,017})Si_{16,263}O_{68}$	$X_{20,954}Y_{9,998}Z_{16,263}O_{68}$	
SGDF-16414	$Ca_{19,834}(Al_{8,611}Fe_{0,324}Mg_{0,987}Mn_{0,030}Ti_{0,012}Cr_{0,001}Zn_{0,001}Ni_{0,009})Si_{16,820}O_{68}$	$X_{19,834}Y_{9,975}Z_{16,820}O_{68}$	
SGDF-16331	$Ca_{13,978}(Al_{13,655}Fe_{1,400}Mg_{0,514}Mn_{0,035}Ti_{0,004}Zn_{0,001}V_{0,001})Si_{15,396}O_{68}$	$X_{13,978}Y_{15,612}Z_{15,399}O_{68}$	
SGDF-16419	$Ca_{19,745}(Al_{8,042}Fe_{0,567}Mg_{1,244}Mn_{0,041}Ti_{0,017}Cr_{0,023}Zn_{0,002}V_{0,002}Ni_{0,003})Si_{16,944}O_{68}$	$X_{19,745}Y_{9,941}Z_{16,944}O_{68}$	
SGDF-16422	$Ca_{20,085}(Al_{8,125}Fe_{0,405}Mg_{1,285}Mn_{0,054}Ti_{0,006}Cr_{0,003}Zn_{0,001}V_{0,001}Ni_{0,002})Si_{16,851}O_{68}$	$X_{20,085}Y_{9,882}Z_{16,851}O_{68}$	
SGDF-16425	$Ca_{19,555}(Al_{9,080}Fe_{0,438}Mg_{0,538}Mn_{0,027}Ti_{0,006}Cr_{0,023}V_{0,002}Ni_{0,001})Si_{16,750}O_{68}$	$X_{19,555}Y_{10,113}Z_{16,750}O_{68}$	
SGDF-16417	$Ca_{18,366}(Al_{8,379}Fe_{0,572}Mg_{1,403}Mn_{0,037}Ti_{0,010}Cr_{0,001}Zn_{0,001}V_{0,001}Ni_{0,001})Si_{17,347}O_{68}$	$X_{18,366}Y_{10,405}Z_{17,347}O_{68}$	
SGDF-16418	$Ca_{19,075}(Al_{8,606}Fe_{0,458}Mg_{1,038}Mn_{0,020}Ti_{0,022}Cr_{0,007}Zn_{0,001}V_{0,001}Ni_{0,004})Si_{17,085}O_{68}$	$X_{19,075}Y_{10,157}Z_{17,085}O_{68}$	
SGDF-16317	$Ca_{16,329}(Al_{9,141}Fe_{0,632}Mg_{1,570}Mn_{0,022}Ti_{0,022}Cr_{0,057}V_{0,003}Ni_{0,004})Si_{17,629}O_{68}$	$X_{16,329}Y_{11,451}Z_{17,629}O_{68}$	
SGDF-16427	$Ca_{25,038}(Al_{8,047}Fe_{0,266}Mg_{0,552}Mn_{0,082}Ti_{0,001}Cr_{0,001}Zn_{0,004}Ni_{0,002})Si_{14,900}O_{68}$ **or** $Ca_{4,419}Al_{1,420}Si_{2,629}O_{12}$	$X_{25,038}Y_{8,955}Z_{14,900}O_{68}$	$Ca_{4,419}Al_{1,420}Si_{2,629}O_{12}$
SGDF-16272	$Ca_{18,296}(Al_{8,189}Fe_{1,397}Mg_{1,012}Mn_{0,030}Ti_{0,001}Zn_{0,001}V_{0,001}Ni_{0,001})Si_{17,120}O_{68}$	$X_{18,296}Y_{10,632}Z_{17,120}O_{68}$	
SGDF-16416	$Ca_{19,674}(Al_{7,905}Fe_{0,724}Mg_{1,295}Mn_{0,025}Ti_{0,012}Cr_{0,002}V_{0,001}Ni_{0,002})Si_{16,96}O_{68}$	$X_{19,674}Y_{9,966}Z_{16,96}O_{68}$	